Fictitious spin-$\frac{1}{2}$ operators and multitransition nuclear relaxation in solids: General theory

D. Petit and J.-P. Korb
Laboratoire de Physique de la Matière Condensée, Ecole Polytechnique, 91128 Palaiseau, France
(Received 22 June 1987)

The fictitious spin-$\frac{1}{2}$ operator formalism is used to describe the nuclear relaxation of spins $I > \frac{1}{2}$ in solids for single or mixed relaxation processes. This permits us to describe the time evolution of the nuclear magnetization with a macroscopic kinetic equation extremely convenient for analyzing NMR data. Applications to the spin-spin and spin-lattice relaxations are given for quadrupolar ($I = \frac{3}{2}$) and/or dipolar fluctuations for like ($I = \frac{3}{2}$) and unlike ($I = \frac{3}{2}$, $S \geq \frac{1}{2}$) spins. In these calculations we have purposely chosen an exponential correlation function for all these fluctuating interactions to clearly point out the quantum behavior of the spin system. For quadrupolar relaxation, we predict a narrowing of the central line and a very large broadening of the satellite lines at sufficiently low temperature ($\tau_c \gg 1/\omega_0$). We explain this seemingly paradoxical result by the nonexistence of the adiabatic part in the T_2 process for the central line of a half-integer spin $I > \frac{1}{2}$. Our treatment takes into account the second-order dynamical shifts, which are, in some temperature range, of the same order of magnitude and even much greater than the homogeneous linewidths. Consequently, in the central line, exists an inherent structure or differential line shifts in the lines, respectively, in the absence or in the presence of a residual static quadrupolar interaction. We find a nonexponential time evolution of the longitudinal magnetization coming from a cross relaxation between different spin states. For dipolar relaxation (unlike spins I,S) we predict that such cross relaxation dominates largely, at low temperature, over the direct relaxation and enhances the T_1^{-1} by a factor $\omega_I/(\omega_I - \omega_S)$. We have also studied the general case of quadrupolar and dipolar (like and unlike spins) relaxations. The occurrence of several distinct maxima in the temperature variation of the longitudinal relaxation rates comes from the quantum characteristic frequencies of the spin system (i.e., ω_I, ω_S, $\omega_I - \omega_S$, ω_Q, . . .) rather than by using different *ad hoc* correlation times. The objective of the general theory proposed is indeed to interpret, with a single calculation, all the phenomena induced by the relaxation, including the residual nonaveraged static interaction always present in anisotropic motions. The effects of a residual quadrupolar interaction have been considered explicitly for quadrupolar and dipolar fluctuations. Finally, we have considered the quadrupolar relaxation of the double- and triple-quantum spectra. We show that the double-quantum spectra are composed of two lines whose temperature behavior is similar to that of the satellites in the monoquantum spectra, while the triple-quantum spectra has a temperature behavior similar to the central line of the single-quantum spectra. The theoretical results appear to be directly applicable for analyzing relaxation data for quadrupolar nuclear spins involving anisotropic motions in solids.

I. INTRODUCTION

Solid-state NMR has for many years been used in the study of complex materials.[1-4] However, difficulties still remain in obtaining dynamical information on these systems, especially in presence of nuclear spins $I > \frac{1}{2}$.

From a theoretical point of view these difficulties come mainly from the spin relaxation theory needed to interpret the data. Since the pioneering works of Kubo,[5] Abragam,[6(a)] and Redfield[7] several attempts have been proposed to study the relaxation of such quadrupolar nuclei in solids.[8-12] But these theoretical attempts do not appear able to account for *all* the relevant physical observables induced by the relaxation in *a single unified theory easy to apply*. Such difficulties occur mainly from the complexity of solving the master equation for the spin density matrix[7,13,14] which describes the relaxation for quadrupolar, dipolar or mixed fluctuations. Abragam has proposed a method to avoid such difficulties by giving the relaxation rates through a macroscopic kinetic equation.[6(a)] However, its method was not able to describe all the relaxation cases.[6(b)]

The purpose of this first paper is precisely to generalize the method of Abragam[6(a)] to all the possible fluctuations using the fictitious spin-$\frac{1}{2}$ operator formalism.[3,15,16] We present a reasonably simple application of this formalism to the study of the microdynamics of quadrupolar and/or dipolar nuclei in solids. Here the main difficulty arises in the treatment of the nuclear relaxation due to different mixed fluctuating interactions Λ. The macroscopic kinetic differential equations will be presented for any observable $\langle Q \rangle$ expanded as a vector like $\langle \mathbf{Q} \rangle$ on a complete basis set of $4I(I+1)$ independent fictitious spin-$\frac{1}{2}$ operators I_r^{cd} ($r = x,y,z$) with integers $c < d$ labeling the $2I+1$ Zeeman states. Then for each mechanism of relaxation Λ, the time evolution of

an individual average operator $\langle I_r^{cd} \rangle$ is given in terms of either a spin lattice $1/T_{1\Lambda}^{cd,ef}$ (for $r=z$) or a spin spin $1/T_{2\Lambda}^{cd,ef}$ (for $r=x,y$) component of relaxation rates. Here cd,ef is a notation to specify the coupling behavior of difference of populations (for $1/T_1$) or transitions (for $1/T_2$) between the Zeeman states c,d and e,f. The time evolution of the vector-like $\langle \mathbf{Q} \rangle$ is thus given in terms of a generalized matrix of relaxation $[1/\mathbf{T}_1^{\Lambda}]$ or $[1/\mathbf{T}_2^{\Lambda}]$. The dimension of this matrix is associated to the z or x,y subsets of the basis for $1/T_1$ and $1/T_2$, respectively. In most cases the eigenvalues of this matrix gives information on both the observable relaxation rates and line shapes. In presence of mixing of different mechanisms of relaxation ($\Lambda \neq \Lambda'$), the elements of the total matrix of relaxation are simply obtained by adding the individual matrix elements in the corresponding basis subset.

In Sec. II, we show how to obtain a generalized macroscopic differential equation for any observable using the fictitious spin-$\frac{1}{2}$ operator formalism. The definitions and useful properties of these operators are resumed in two tables. We separate the intercorrelations between different mechanisms $\Lambda \neq \Lambda'$ from the sum of the autocorrelations of these mechanisms. We discuss the conditions of validity of the secular hypothesis for solids where the presence of anisotropies of the local fields is the commonly encountered case. The theoretical treatment of a residual nonaveraged perturbation term $\bar{H}$ is given. This could affect the relaxation when its amplitude is at least of the same order of magnitude as the one inducing the relaxation itself. We will insist particularly on this effect in Sec. IV.

In Sec. III, restricted to the completely averaged case ($\bar{H}=0$), we apply our method to the quadrupolar ($I=\frac{3}{2}$) and dipolar relaxations for like and unlike spins. In each case we present the elements of the matrix of relaxation, in an adapted basis set or subset, in terms of linear combinations of spectral densities at the frequency (or multiple) of the transitions. When it is possible, a comparison with previous results is given. Theoretical diagrams for the temperature variations of the spin-spin and spin-lattice relaxation rates are given for the quadrupolar, dipolar (like and unlike spins). A second-order dynamical line shift is evidenced for these processes. For quadrupolar interaction this induces a temperature dependent structure in the adsorption spectrum even in the completely averaged case. The usefulness of the presented formalism is evidenced in treating explicitly the case of a mixing of quadrupolar and dipolar (like and unlike spins) fluctuations. The temperature variations of the spin-spin and spin-lattice relaxation rates are presented and discussed in such mixing cases which occur in real materials. A surprising result is the occurrence of several distinct maxima in the temperature dependence of the observable spin-lattice relaxation rates obtained with a single correlation time. As proved in this paper, by choosing on purpose the same monoexponential correlation function for all the fluctuations, this is due to the repartition in the spectral domain of the characteristic frequencies of the transitions created by the various kinds of fluctuations. This shows the importance of a correct treatment of the quantum part of the relaxation process before trying to interpret the dynamics from the data.

In Sec. IV, the effects of a residual quadrupolar interaction have been considered explicitly for quadrupolar and dipolar fluctuations. Finally we have considered the quadrupolar relaxation of the double- and triple-quantum spectra. We show that the double-quantum spectra is composed of two lines whose temperature behavior is similar to one of the satellites in the monoquantum spectra, while the triple-quantum spectra has a temperature behavior similar to the central line of the monoquantum spectra.

The applications of this treatment to some materials of low symmetry, such as the superionic conductors[2,17,18] are reported in a following paper.

II. SEMICLASSICAL TREATMENT OF THE SPIN RELAXATION IN SOLIDS

A. Macroscopic differential equation

The purpose of this section is to propose a general treatment of the spin relaxation for an ensemble of spins $I>\frac{1}{2}$ in solids. For the sake of convenience, we shall follow as close as possible the usual treatments and notations of Abragam[6(a)] and generalize it, when it will be necessary, using the fictitious spin-$\frac{1}{2}$ operator formalism.[15,16]

Let start from the total Hamiltonian

$$H_0+H_1(t)$$

where the constant part H_0 is given by the superposition of a Zeeman term H_z and a time-averaged part $\bar{H}$

$$H_0=H_z+\bar{H} , \tag{1a}$$

with $\bar{H} \ll H_z$ and where the time dependent part $H_1(t)$ given by

$$H_1(t)=H(t)-\bar{H} \tag{1b}$$

represents the deviation from $\bar{H}$. The interest of such partition is to include explicitly a possible non zero time averaged part in the treatment of the relaxation. This is of particular importance for local and long range ionic motions in superionic conductors[17,18] or in polymers studies.[19]

1. *Representation in the interaction frame*

In the following the stationary random operator $H_1(t)$ will be considered as a high-frequency perturbation that can be treated by usual perturbation theory using the well-known master equation for the spin density matrix[6(a),13]

$$\frac{d}{dt}\sigma^*(t)=-\int_0^t d\tau \overline{[H_1^*(t),[H_1^*(t-\tau),\sigma^*(t)-\sigma_0]]} \tag{2}$$

where the overbar stands for a statistical average over the system of spins and where $\sigma^*(t)$ and $H_1^*(t)$ are defined in the interaction representation by

$$\sigma^*(t)=e^{iH_0t}\sigma(t)e^{-iH_0t} , \tag{3a}$$

$$H_1^*(t)=e^{iH_0t}H_1(t)e^{-iH_0t}\ , \tag{3b}$$

and σ_0 is the equilibrium density matrix. It is recalled that Eq. (2) is valid providing the conditions

$$\tau_c \ll t \ll \overline{(|H_1|^2\tau_c)^{-1}}\ , \tag{3c}$$

where τ_c is a time cut off for the correlation functions involved in such master equation and t is supposed much larger than τ_c but much shorter than an estimate of the homogeneous relaxation time. From Eqs. (2) and (3c), we can derive the macroscopic differential equation of any time independent observable Q like I_x, I_y, I_z in the interaction representation as

$$\frac{d}{dt}\langle Q\rangle^* \equiv \mathrm{Tr}\left[Q\frac{d}{dt}\sigma^*(t)\right] = -\int_0^\infty d\tau\,\mathrm{Tr}\overline{\{[H_1^*(t-\tau),[H_1^*(t),Q]][\sigma^*(t)-\sigma_0]\}}\ . \tag{4}$$

The possibility of transforming Eq. (4) into a kinetic equation

$$\frac{d}{dt}\langle Q\rangle^* \equiv -\frac{1}{T_i}(\langle Q\rangle^* - \langle Q\rangle_0)\ , \tag{5}$$

which defines a relaxation time T_i, could avoid the explicit calculation of the time evolution of the density matrix. However, this latter transformation is not always possible[6(b)] due to the fact that for $I \neq \frac{1}{2}$ the operators I_x, I_y, and I_z do not belong to a complete basis. On the contrary, the fictitious spin-$\frac{1}{2}$ operator formalism[15] allows to define such a basis. This latter is built on a set of $4I(I+1)$ spin operators I_r^{cd}, where $r=x,y,z$ and the integer indices $c<d\in\{1,\ldots,2I+1\}$ stand for the eigenstates $m\in\{I,I-1,\ldots,-I\}$ of the Zeeman Hamiltonian, respectively. We point out below the orthogonality relations and the definition of the scalar product for the spin operators which compose the basis. For r (or s)$=x,y$ such orthogonality relation is given by

$$\mathrm{Tr}\{I_r^{cd}I_s^{ef}\} = \tfrac{1}{2}\delta_{rs}\delta_{ce}\delta_{df}\ . \tag{6a}$$

For r and $s=z$, there is a redundance of the I_z^{cd} operators in the z subspace, so we restrict the choice of such operators according to the relation

$$\mathrm{Tr}\{I_z^{cd}I_z^{ef}\} = \tfrac{1}{2}\delta_{ce}\delta_{df}\ . \tag{6b}$$

Then one can express the operator Q as

$$Q = a_0\mathbf{1} + \sum_r \sum_{c<d} q_r^{cd}I_r^{cd}\ , \tag{6c}$$

where $\mathbf{1}$ is the $(2I+1)(2I+1)$ unit matrix and

$$a_0 = \frac{1}{2I+1}\mathrm{Tr}\{Q\},\quad q_r^{cd} = 2\mathrm{Tr}\{QI_r^{cd}\}\ . \tag{6d}$$

Thus q_r^{cd} in Eq. (6c) defines a projection-like of Q on a basis operator I_r^{cd}. For a two-spin (I,S) Hamiltonian $H_1(t)$, Eq. (6c) is always valid if we extend this equation by a direct product of the spin operators I and S. We give in the Table I the definition and some useful properties of such operators.

We intend to prove below that using the spin fictitious algebra, we can always transform Eq. (4) into a generalized kinetic equation

$$\frac{d}{dt}\langle \mathbf{Q}\rangle^* = -\left[\frac{1}{\mathbf{T}_i}\right](\langle \mathbf{Q}\rangle^* - \langle \mathbf{Q}\rangle_0)\ , \tag{7}$$

where the vectorial $\langle \mathbf{Q}\rangle^*$ and matrix $[1/\mathbf{T}_i]$ notations will be defined in the following sections.

Substituting Eq. (6c) into Eq. (4) gives for each operator I_r^{cd} a macroscopic differential equation

$$\frac{d}{dt}\langle I_r^{cd}\rangle^* = -\int_0^\infty d\tau\,\mathrm{Tr}\overline{\{[H_1^*(t),[H_1^*(t-\tau),I_r^{cd}]][\sigma^*(t)-\sigma_0]\}}\ . \tag{8}$$

TABLE I. Definition and useful properties of fictitious spin-$\frac{1}{2}$ operators.

$\langle c\,|\,I_x^{cd}\,|\,d\rangle = \langle d\,|\,I_x^{cd}\,|\,c\rangle = \frac{1}{2}$
$\langle c\,|\,I_y^{cd}\,|\,d\rangle = -\langle d\,|\,I_y^{cd}\,|\,c\rangle = -\frac{i}{2}$
$\langle c\,|\,I_z^{cd}\,|\,c\rangle = -\langle d\,|\,I_z^{cd}\,|\,d\rangle = \frac{1}{2}$, all the other elements are equal to zero
$I_\pm^{cd} = I_x^{cd} \pm iI_y^{cd}$
$I_z^{cd} = I_z^{ce} + I_z^{ed}$

TABLE II. Commutation rules for the spin-$\frac{1}{2}$ operators.

$[I_\pm^{ij}, I_x^{ij}] = \pm I_z^{ij},\ [I_x^{ij}, I_y^{ij}] = iI_z^{ij},\ [I_+^{ij}, I_-^{ij}] = 2I_z^{ij},$
$[I_\pm^{ij}, I_y^{ij}] = iI_z^{ij},\ [I_{x/y}^{ij}, I_{x/y}^{jk}] = \pm\frac{i}{2}I_y^{ik},\ [I_\pm^{ij}, I_\pm^{jk}] = \pm I_\pm^{ik},$
$[I_\pm^{ij}, I_z^{ij}] = \mp I_\pm^{ij},\ [I_x^{ij}, I_y^{jk}] = -\frac{i}{2}I_x^{ik},\ [I_\pm^{ij}, I_\mp^{ik}] = 0,$
$[I_\pm^{ij}, I_x^{jk}] = \pm\frac{1}{2}I_\pm^{ik},\ [I_{x/y}^{ij}, I_z^{jk}] = \pm\frac{i}{2}I_{y/x}^{ij},$
$[I_\pm^{ij}, I_y^{jk}] = -\frac{i}{2}I_\pm^{ik},\ [I_z^{ij}, I_z^{jk}] = 0,$
$[I_\pm^{ij}, I_z^{jk}] = \pm\frac{1}{2}I_\pm^{ij},\ [I_p^{ij}, I_z^{ik} + I_z^{jk}] = 0,$

In the most general case the fluctuating perturbation $H_1(t)$ can be written as a superposition of different interactions $H_\Lambda(t)$

$$H_1(t)=\sum_\Lambda H_\Lambda(t) \ . \tag{9a}$$

Each interaction Λ can be expressed as a scalar product of spatial spherical tensor $F^\Lambda(t)$ and spin spherical tensor A^Λ

$$H_\Lambda(t)=C_\Lambda \sum_{l=0}^{2} \sum_{m=-l}^{+l} (-1)^m F^\Lambda_{l-m}(t) A^\Lambda_{lm} \ , \tag{9b}$$

where C_Λ is a numerical factor.

In the interaction representation each component $\mathbf{A}^\Lambda_{lm}$ becomes

$$e^{iH_0 t} A^\Lambda_{lm} e^{-iH_0 t}=\sum_p A^{\Lambda p}_{lm} \exp(i\omega^{\Lambda p}_{lm} t) \ , \tag{10}$$

where the index p stands for the different transition frequencies. With Eqs. (9,10), one obtains for Eq. (8)

$$\frac{d}{dt}\langle I^{cd}_r\rangle^* = -\sum_{\Lambda,\Lambda'} C_\Lambda C_{\Lambda'} \sum_{l,l'} \sum_{m,m'} (-1)^{m+m'} \sum_{p,p'} \exp\{i[(\omega^{\Lambda p}_{lm}+\omega^{\Lambda' p'}_{l'm'})]_{\text{restr}} t\}$$
$$\times \int_0^\infty d\tau \, \overline{F^\Lambda_{l-m}(0) F^{\Lambda'}_{l'-m'}(\tau)} \exp(-i\omega^{\Lambda p}_{lm}\tau)$$
$$\times \mathrm{Tr}\{[A^{\Lambda p}_{lm},[A^{\Lambda' p'}_{l'm'},I^{cd}_r]][\sigma^*(t)-\sigma_0]\} \ . \tag{11}$$

We will see in Sec. II B that the only time-dependent terms conserved in Eq. (11) will be those (noted $[\ ]_{\text{restr}}$) coming from the non zero time averaged part of the perturbation $\bar{H}$ which induce a very slow time oscillating contribution for which all the coefficients of Eq. (11) stay constant when t verifies Eq. (3c). Using Eqs. (6c) and (6d) and the commutation rules given in Table II, the double commutator in Eq. (11) can be written as

$$[A^{\Lambda p}_{lm},[A^{\Lambda' p'}_{l'm'},I^{cd}_r]]=\sum_s \sum_{\substack{e,f \\ e<f}} a^{\alpha\beta}_{uv} I^{ef}_s \ , \tag{12a}$$

with

$$a^{\alpha\beta}_{uv}=2\,\mathrm{Tr}\{[A^{\Lambda p}_{lm},[A^{\Lambda' p'}_{l'm'},I^{cd}_r]]I^{ef}_s\} \ , \tag{12b}$$

and the collective indices α, β, u and v symbolize four indices, respectively

$$\alpha=(^{\Lambda p}_{lm}), \quad \beta=(^{\Lambda' p'}_{l'm'}), \quad u=(^{cd}_{r}), \quad v=(^{ef}_{s}) \ . \tag{12c}$$

Substituting Eq. (12a) into the rhs of Eq. (11) gives for the Trace

$$\sum_s \sum_{\substack{e,f \\ e<f}} a^{\alpha\beta}_{uv} \mathrm{Tr}\{I^{ef}_s[\sigma^*(t)-\sigma_0]\} \equiv \sum_s \sum_{\substack{e,f \\ e<f}} a^{\alpha\beta}_{uv}\{\langle I^{ef}_s\rangle^* - \langle I^{ef}_s\rangle_0\} \ . \tag{13}$$

Finally for Eq. (11)

$$\frac{d}{dt}\langle I^{cd}_r\rangle^* = -\sum_s \sum_{\substack{e,f \\ e<f}} \frac{1}{T^{uv}_i}\{\langle I^{ef}_s\rangle^* - \langle I^{ef}_s\rangle_0\} \ , \tag{14a}$$

where

$$\frac{1}{T^{uv}_i} = \sum_{\Lambda,\Lambda'} C_\Lambda C_{\Lambda'} \sum_{l,l'} \sum_{m,m'} (-1)^{m+m'} \sum_{p,p'} \exp\{i[(\omega^{\Lambda p}_{lm}+\omega^{\Lambda' p'}_{l'm'})]_{\text{rest}} t\} a^{\alpha\beta}_{uv} \int_0^\infty d\tau \, \overline{F^\Lambda_{l-m}(0) F^{\Lambda'}_{l'-m'}(\tau)} \exp(-i\omega^{\Lambda p}_{lm}\tau) \ . \tag{14b}$$

Now Eq. (14a) defines a kinetic equation of *one* component of a vector $\langle \mathbf{Q}\rangle^*$ built on the basis of $4I(I+1)$ independent fictitious spin-$\frac{1}{2}$ operators; the elements of the relaxation matrix $[1/\mathbf{T}_i]$ being given by Eq. (14b). Therefore, without introducing physical restrictions, one can always write Eq. (14) into the form given in Eq. (7).

2. *Representation into the rotating frame*

In liquids the interaction representation corresponds to the rotating frame at the resonance frequency. In solids, when $\bar{H}\neq 0$, these latter representations are different and one is usually interested by the dynamical response in the rotating frame. In Table III, one introduces the definitions and some useful relations to express the observables and their dynamics in different frames.

Using the dynamical transformation given in Table III with $Q\equiv I^{cd}_r$, one has in the rotating frame

$$\frac{d}{dt}\langle \tilde{I}^{cd}_r\rangle = -i \sum_{s,e<f} \bar{\omega}_{r^{cd}s^{ef}}(\langle I^{ef}_s\rangle^* - \langle I^{ef}_s\rangle_0) + \frac{d}{dt}\langle \tilde{I}^{cd}_r\rangle^* \ , \tag{15a}$$

TABLE III. Observables in different representations.

Interaction	Q^* time independent	σ^*	$\langle Q\rangle^* \equiv \mathrm{Tr}\{Q^*\sigma^*\}$
Rotating	$\tilde{Q}\equiv e^{-i\bar{H}t}Q^*e^{+i\bar{H}t}$	$\tilde{\sigma}\equiv e^{-i\bar{H}t}\sigma^*e^{+i\bar{H}t}$	$\langle Q\rangle^{\sim} \equiv \mathrm{Tr}\{\tilde{Q}\tilde{\sigma}\}$
Laboratory	$Q\equiv e^{-iH_0t}Q^*e^{+iH_0t}$	$\sigma\equiv e^{-iH_0t}\sigma^*e^{+iH_0t}$	$\langle Q\rangle \equiv \mathrm{Tr}\{Q\sigma\}$
			all equal

with the dynamical transformation:

$$\frac{d}{dt}\langle\tilde{Q}\rangle \equiv \mathrm{Tr}\left[\tilde{Q}\left[\frac{d\tilde{\sigma}}{dt}\right]\right] = -i\,\mathrm{Tr}[(Q^*,\bar{H})\sigma^*] + \frac{d}{dt}\langle Q\rangle^* \neq \frac{d}{dt}\langle Q\rangle^{\sim}$$

where $\frac{d}{dt}\langle Q\rangle^* = \frac{d}{dt}\langle Q^*\rangle$

where according to Eq. (6), the $\bar{\omega}_{r^{cd}s^{ef}}$ given by

$$\bar{\omega}_{r^{cd}s^{ef}} = 2\,\mathrm{Tr}[[I_r^{cd},\bar{H}]I_s^{ef}] \,, \tag{15b}$$

represent the characteristic splitting frequencies of the spectrum. In the following we will consider only the secular part of the perturbation $\bar{H}$ (i.e., $[\bar{H},H_Z]=0$), for instance, the first-order quadrupolar interaction $\bar{H}=H_Q$. This corresponds to omit the fast oscillating terms in the relaxation treatment.[6(a),13]

B. Autocorrelations and intercorrelations

The expression (14b) for the relaxation rates both includes the autocorrelation and intercorrelation terms either for different interactions or individual tensorial components of a given interaction. These intercorrelation terms can be simplified for a liquid owing to the orthogonality properties of irreducible tensors and of the isotropical character of the motion. However in solids the motions are mostly anisotropic and these intercorrelation terms should be included.

Let separate Eqs. (14) according to the following three steps. (i) We separate the intercorrelations between different interactions from the sum of autocorrelations of these interactions. (ii) We discuss the secular hypothesis in order to conserve only the slow variation component into Eq. (14). (iii) For a given interaction, we discuss the case of the intercorrelations between different irreducible tensorial components.

The first step (i) gives for Eqs. (14) [generalized as Eq. (7)]

$$\frac{d}{dt}\langle Q\rangle^* = -\left[\sum_{\Lambda}\left[\frac{1}{T_i^{\Lambda}}\right] + \tfrac{1}{2}\sum_{\Lambda\neq\Lambda'}\left[\frac{1}{T_i^{\Lambda\Lambda'}}\right]\right]\{\langle Q\rangle^* - \langle Q\rangle_0\} \,. \tag{16}$$

This first sum of matrices in the rhs of Eq. (16) reveals the statistical independence of the autocorrelation contribution of each interaction Λ contrary to the second sum which takes into account a possible intercorrelation between two different interactions Λ and Λ'. This intercorrelation effect, often neglected in the literature, could occur in solids, for instance, when a nucleus is both sensitive to chemical shift, quadrupolar and dipolar interactions. For example, when such a nucleus jumps between two sites, the chemical shift and electrical field gradient variations are simultaneous and then temporarily correlated. This type of event occurs in solids and consequently renders such a temporary correlation statistically non-negligible. We shall continue only with the first sum in Eq. (16), though both terms could be formally treated in the same way.

Step (ii) is relative to the consideration of the secular terms in Eq. (14). Owing to the definition of H_0, where $\bar{H}$ is always a perturbation compared to H_Z, one conserves only the terms with $m'=-m$. Moreover among the remaining p',p'' time dependent terms we conserve only those for which

$$[\,|\,\omega_{lm}^{p'}+\omega_{l'-m}^{p''}\,|\,]_{\mathrm{restr}} \equiv |\,\Omega_{ll'm}^{p'p''}\,| \geq \overline{|\,H_1^2\,|}\,\tau_c \,. \tag{17a}$$

It is particularly important to conserve such terms because their frequency Ω, coming from $\bar{H}$, are not necessarily much larger than the homogeneous relaxation time. Consequently they will give a nonnegligible time dependent contribution in Eq. (14). However these terms should also verify Eq. (3c), thus giving the following restrictive condition on t and Ω:

$$\tau_c \ll t \ll (\Omega_{ll'm}^{p'p''})^{-1} \leq \overline{(|\,H_1\,|^2\tau_c)^{-1}} \,, \tag{17b}$$

which transforms such time dependence in a very slow oscillation, thus preserving the kinetic character of Eq. (14). Similar restrictions have been previously considered when dealing with the solidlike contribution of the nonzero average dipolar coupling to NMR signals.[19]

Step (iii) concerns the possible intercorrelations between different l components of $F_{lm}(t)$, defined in Eq. (9b), for a given interaction Λ. This step is not relevant for the quadrupolar ($\Lambda=Q$) and dipolar ($\Lambda=D$) interactions because $l=l'=2$. On the other hand, chemical shift ($\Lambda=\sigma$), J-coupling ($\Lambda=J$) and spin-rotation ($\Lambda=SR$) interactions can produce such intercorrelations. From a theoretical point of view these kinds of intercorrelations should be conserved in solids because of the anisotropy of the angular distribution probability.

According to these three steps, a matrix relaxation element can be written as

$$\frac{1}{T^{uv}_{i\Lambda}}=C^2_\Lambda\sum_{ll'}\sum_m(-1)^m\sum_{pp'}2\,\mathrm{Tr}\{[A^p_{lm},[A^{p'}_{l'-m},I_u]]I_v\}\exp[i(\Omega^{pp'}_{ll'm}t)_{\mathrm{restr}}]G_{ll'm}(0)[\tfrac{1}{2}j_{ll'm}(\omega^p_{lm})-ik_{ll'm}(\omega^p_{lm})]\ , \tag{18}$$

where the notation $[\ ]_{\mathrm{restr}}$ stands for the restrictions for Ω and t given in Eq. (17b). One introduces here the reduced and nonreduced spectral densities j and J, respectively, by

$$j_{ll'm}(\omega^p_{lm})\equiv\int_{-\infty}^{+\infty}g_{ll'm}(\tau)\exp(-i\omega^p_{lm}\tau)d\tau\ ,$$

$$J_{ll'm}(\omega^p_{lm})=G_{ll'm}(0)j_{ll'm}(\omega^p_{lm}) \tag{19a}$$

$$k_{ll'm}(\omega^p_{lm})\equiv\int_0^{+\infty}g_{ll'm}(\tau)\sin(\omega^p_{lm}\tau)d\tau\ ,$$

$$K_{ll'm}(\omega^p_{lm})=G_{ll'm}(0)k_{ll'm}(\omega^p_{lm}) \tag{19b}$$

and the reduced correlation functions

$$g_{ll'm}(\tau)\equiv\overline{F_{lm}(0)F^*_{l'm}(\tau)}/G_{ll'm}(0)\ , \tag{19c}$$

with

$$G_{ll'm}(0)\equiv\overline{F_{lm}(0)F^*_{l'm}(0)}\ . \tag{19d}$$

The reduced spectral density $k(\omega)$ defined in Eq. (19b) induces a previously studied dynamical shift of the resonance lines.[20,21]

III. APPLICATION TO QUADRUPOLAR AND DIPOLAR RELAXATIONS WITHOUT A RESIDUAL TIME AVERAGED INTERACTION

The cases where $\bar{H}\neq0$ will be treated in Sec. IV. Here we restrict to the case $\bar{H}=0$ for quadrupolar and dipolar fluctuations in order to illustrate the efficiency of the proposed formalism in some simple but useful cases. Basically the interest in these cases is twofold. First, we both obtain with the same treatment, the spin-lattice relaxation time T_1 and the spin-spin relaxation time T_2 for quadrupolar relaxation. This result is achieved in a wider range of correlation times ($1/\omega_0\leq\tau_c\leq1/H_1$) than in the extreme motional narrowing ($\tau_c\ll1/\omega_0$) previously done.[6(a),22] Second, we present the only way to superpose properly the quadrupolar and dipolar relaxation mechanisms by adding our generalized relaxation matrices.

In order to illustrate the different variations of the observables, we have considered below in the applications and on the figures, monoexponential correlation functions with a correlation time characteristic of an activation law: $\tau_c=\tau_0\exp(E_a/kT)$ with $\tau_0=7.5\times10^{-12}$ sec and $E_a=0.215$ eV. These values and those for the quadrupolar and dipolar fluctuation amplitudes given in the legends of the figures correspond to a case of a superionic conductor.[17] Of course it is always possible to have other forms of correlation functions depending on the physical case considered, for instance when one considers translational motions in low-dimensional systems.[2,23]

A. Single source of relaxation

1. *Quadrupolar relaxation*

We consider the relaxation of a single nuclear species with $I=\frac{3}{2}$ in the presence of a strong constant magnetic field $\mathbf{B}_0$. We study the case where the relaxation is only due to the modulation of the quadrupolar interaction ($\Lambda=Q$). Physically this case applies for an isotropic liquid. However one should notice that the monoexponential description for the correlation function is not adapted to real liquids.[24,25] Here one has

$$H_0=H_Z=\omega_I I_Z\ , \tag{20a}$$

$$H_1(t)=H_Q(t)\ , \tag{20b}$$

where $\omega_I=-\gamma_I B^z_0$. According to Eq. (9b) in which $l=2$, the modulation of the quadrupolar interaction can be written as

$$H_Q(t)=C_Q\sum_{m=-2}^{+2}[F_m(t)]^*A_m\ , \tag{21}$$

where $C_Q=eQ/2I(2I-1)\hbar$ with Q is the nuclear quadrupole moment and eq is the Z component of the electrical field gradient (efg). It is worthwhile to express each component F_m in function of the component $\mathcal{F}_{m'}$ into the principal axis **XYZ** of the electrical field gradient (efg)

$$F_m=\sum_{m'=-2}^{+2}D^{(2)}_{m'm}(\alpha,-\theta,-\phi)\mathcal{F}_{m'}\ , \tag{22}$$

where

$$\mathcal{F}_0=\sqrt{\tfrac{3}{2}}\delta_Q,\quad \mathcal{F}_{\pm1}=0,\quad \mathcal{F}_{\pm2}=\tfrac{1}{2}\eta_Q\delta_Q\ , \tag{23a}$$

introducing the usual notations for quadrupolar interactions

$$\delta_Q\equiv V_{ZZ}\equiv eq,\quad \eta_Q\equiv\left[\frac{V_{YY}-V_{XX}}{V_{ZZ}}\right]\ . \tag{23b}$$

In Eq. (22) we used the Wigner matrix $D^{(2)}(\alpha,-\theta,-\phi)$ (Ref. 26) which rotates the principal axis **X,Y,Z** of the efg into the corresponding axis **x,y,z** of the laboratory frame. The angles θ and ϕ are the spherical coordinates describing the **Z** axis of the efg in the laboratory frame. The angle α is defined by the rotation around **Z** which brings the principal axis **X** into the (**z,Z**) plane.

Now we express the spin spherical tensor A in a fictitious spin-$\frac{1}{2}$ basis $\{I^{cd}_r\}$. For that we associate the $2I+1$ indices c (or d)$=1,2,3,4$ to the spin states $m=\frac{3}{2}$, $\frac{1}{2}$, $-\frac{1}{2}$, and $-\frac{3}{2}$, respectively. The basis operators I^{cd}_r should verify the Eqs. (6). In particular to avoid the redundance of the I^{cd}_z subset of the basis we choose the three operators $I^{14}_z, I^{23}_z, (1/\sqrt{2})(I^{12}_z-I^{34}_z)$ which verify Eq. (6b).

Then the A components can be written, after some algebraic manipulations using Table I, as

$$A_0=\frac{1}{\sqrt{6}}(3I_z^2-I(I+1)=\sqrt{6}(I_z^{12}-I_z^{34}) , \tag{24a}$$

$$A_{\pm 1}=\mp\tfrac{1}{2}(I_zI_\pm+I_\pm I_z)=\mp\sqrt{3}(I_\pm^{12}-I_\pm^{34}) , \tag{24b}$$

$$A_{\pm 2}=\tfrac{1}{2}I_\pm^2=\sqrt{3}(I_\pm^{13}+I_\pm^{24}) . \tag{24c}$$

In the interaction representation Eq. (10) reduces to

$$e^{iH_0t}A_me^{-iH_0t}=A_me^{im\omega_I t} , \tag{25}$$

with $\omega_m=m\omega_I$.

a. Spin-lattice relaxation. To obtain the matrix of relaxation describing the time evolution towards equilibrium of the longitudinal magnetization, one has to replace I_u in Eq. (18) by the three operators $I_z^{14},I_z^{23},(1/\sqrt{2})(I_z^{12}-I_z^{34})$. Using the commutating relations given in Appendix A, one has the following longitudinal kinetic equations:

$$\frac{d}{dt}\begin{bmatrix}\langle I_z^{14}\rangle^* \\ \langle I_z^{23}\rangle^* \\ \frac{1}{\sqrt{2}}(\langle I_z^{12}\rangle-\langle I_z^{34}\rangle)^*\end{bmatrix}=-\begin{bmatrix}\frac{1}{T_{1Q}^{14,14}} & \frac{1}{T_{1Q}^{14,23}} & 0 \\ \frac{1}{T_{1Q}^{23,14}} & \frac{1}{T_{1Q}^{23,23}} & 0 \\ 0 & 0 & \frac{1}{T_{1Q}^{12-34,12-34}}\end{bmatrix}\begin{bmatrix}\Delta\langle I_z^{14}\rangle^* \\ \Delta\langle I_z^{23}\rangle^* \\ \frac{\Delta}{\sqrt{2}}(\langle I_z^{12}\rangle-\langle I_z^{34}\rangle)^*\end{bmatrix} \tag{26}$$

where the spin lattice relaxation rates are given in Table IV and with the notations: $\Delta\langle I_z^{c-d}\rangle^*$ for $\langle I_z^{cd}\rangle^*-\langle I_z^{cd}\rangle_0$.

From this relaxation matrix one notes that the component $(\langle I_z^{12}\rangle-I_z^{34}\rangle)^*$ relaxes independently of the other components. Then it represents an eigenstate of the longitudinal relaxation matrix. Along these lines, one can find easily the other two eigenstates and transforms the Eq. (26) into three decoupled kinetic equations:

$$\frac{d}{dt}(\langle I_z^{14}\rangle^*+\langle I_z^{23}\rangle^*)=-\frac{1}{T_{1Q}^A}\Delta(\langle I_z^{14}\rangle^*+\langle I_z^{23}\rangle^*) ,$$

$$\frac{d}{dt}(\langle I_z^{14}\rangle^*-\langle I_z^{23}\rangle^*)=-\frac{1}{T_{1Q}^B}\Delta(\langle I_z^{14}\rangle^*-\langle I_z^{23}\rangle^*) ,$$

$$\frac{d}{dt}(\langle I_z^{12}\rangle^*-\langle I_z^{34}\rangle^*)=-\frac{1}{T_{1Q}^C}\Delta(\langle I_z^{12}\rangle^*-\langle I_z^{34}\rangle^*) , \tag{27}$$

where

TABLE IV. Elements of spin-lattice relaxation rates for the quadrupolar case.

$$\frac{1}{T_{1Q}^{cd,ef}}=3C_Q^2[aJ_1(\omega_I)+bJ_2(2\omega_I)]$$

cd,ef	a	b
14,14	1	1
14,23	−1	1
23,14=14,23		
23,23=14,14		
12-34,12-34	2	2

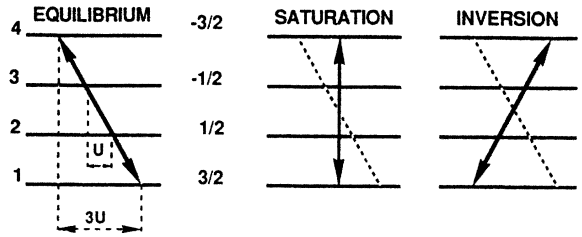

Deviation from equilibrium in unit of u	Equilibrium	Saturation	Inversion	Symbols
$\Delta<I_z^{14}>^*$	0	3	6	x
$\Delta<I_z^{23}>^*$	0	1	2	x
$\Delta(<I_z^{12}>^*-<I_z^{34}>^*)$	0	0	0	x + o
$\Delta(<I_z^{14}>^*+<I_z^{23}>^*)$	0	4	8	+
$\Delta(<I_z^{14}>^*-<I_z^{23}>^*)$	0	2	4	+
$\Delta(3<I_z^{14}>^*+<I_z^{23}>^*)$	0	10	20	o
$\Delta(<I_z^{14}>^*-3<I_z^{23}>^*)$	0	0	0	o

FIG. 1. Schematic diagrams for the deviations Δ from equilibrium of the population differences between levels 14,23, and 12-34 for saturation and inversion preparations. The first diagram presents the different notations and equilibrium offset populations, in unit of $U=(N/8)\hbar\omega_0/kT$, between the levels 14 and 23. The deviations from the equilibrium (dotted lines) are noted in each case by a continuous line. In the last column the symbols (×,+,0) represent the basis of averaged operators used in the calculations of the $[1/\mathbf{T}_1]$ matrices (×), the eigenstates for both quadrupolar (+) and dipolar (0) relaxation processes, respectively.

$$\frac{1}{T_{1Q}^{A}}=6C_Q^2J_2(2\omega_I),\quad \frac{1}{T_{1Q}^{B}}=6C_Q^2J_1(\omega_I)\ ,$$
$$\frac{1}{T_{1Q}^{C}}=\frac{1}{T_{1Q}^{12-34,12-34}}\ . \tag{28}$$

Figure 1 shows that the deviation Δ, at $t=0$, from equilibrium of the population differences between levels 1-4 and 2-3 always belongs to the subspace generated by $\langle I_z^{14}\rangle$ and $\langle I_z^{23}\rangle$ whether for saturation or inversion experiments. In consequence only the first two rates I/T_{1Q}^{A} and I/T_{1Q}^{B} are involved in such experiments. The last one I/T_{1Q}^{C} cannot be measured because the deviation $\Delta(\langle I_z^{12}\rangle-\langle I_z^{34}\rangle)^*$ is always zero.

A comparison with previous calculations,[22] using a master equation for the populations applied in the case of an isotropic rotational diffusion,[6(a)] transforms our results as

$$\frac{1}{T_{1Q}^{A}}=\frac{9}{5}\left[1+\frac{\eta_Q^2}{3}\right]C_Q^2\delta_Q^2j_2(2\omega_I)\equiv 2W_2\ , \tag{29a}$$

$$\frac{1}{T_{1Q}^{B}}=\frac{9}{5}\left[1+\frac{\eta_Q^2}{3}\right]C_Q^2\delta_Q^2j_1(\omega_I)\equiv 2W_1\ , \tag{29b}$$

which are expressed in terms of the well-known relaxation rates W_1 and W_2.[22]

b. Spin-spin relaxation. For the transverse relaxation rates, we replace I_u in Eq. (18) by the three operators $I_\pm^{12}, I_\pm^{23}, I_\pm^{34}$, respectively. Using the commutation rules given in Appendix A, one has the following transverse kinetic equations:

$$\frac{d}{dt}\begin{pmatrix}\langle I_\pm^{12}\rangle^*\\ \langle I_\pm^{23}\rangle^*\\ \langle I_\pm^{34}\rangle^*\end{pmatrix}=-\begin{pmatrix}\frac{1}{T_{2Q}^{12,12}} & 0 & \frac{1}{T_{2Q}^{12,34}}\\ 0 & \frac{1}{T_{2Q}^{23,23}} & 0\\ \frac{1}{T_{2Q}^{34,12}} & 0 & \frac{1}{T_{2Q}^{34,34}}\end{pmatrix}\mp i\begin{pmatrix}\omega_Q^{12} & 0 & 0\\ 0 & \omega_Q^{23} & 0\\ 0 & 0 & \omega_Q^{34}\end{pmatrix}\begin{pmatrix}\langle I_\pm^{12}\rangle^*\\ \langle I_\pm^{23}\rangle^*\\ \langle I_\pm^{34}\rangle^*\end{pmatrix}\ , \tag{30}$$

where the spin spin relaxation rates are given in Table V and the dynamical shifts ω_Q^{cd} are given by

$$\omega_Q^{12}=6C_Q^2K_1(\omega_I)\ ,$$
$$\omega_Q^{23}=6C_Q^2[K_1(\omega_I)+K_2(2\omega_I)]\ , \tag{31}$$
$$\omega_Q^{34}=\omega_Q^{12}\ ,$$

The solution of Eq. (30) in the frequency domain is obtained after some algebraic manipulations, which give for the two observable eigenstates of the relaxation

$$[\langle I_\pm^{12}\rangle^*(\omega)+\langle I_\pm^{34}\rangle^*(\omega)]=\frac{T_{2Q}^{\Sigma}-i(\omega\mp\omega_Q^{12})(T_{2Q}^{\Sigma})^2}{1+[(\omega\mp\omega_Q^{12})(T_{2Q}^{\Sigma})]^2}[\langle I_\pm^{12}(0)\rangle^*+\langle I_\pm^{34}(0)\rangle^*]\ , \tag{32a}$$

$$\langle I_\pm^{23}\rangle^*(\omega)=\frac{T_{2Q}^{23,23}-i(\omega\mp\omega_Q^{23})(T_{2Q}^{23,23})^2}{1+[(\omega\mp\omega_Q^{23})(T_{2Q}^{23,23})]^2}\langle I_\pm^{23}(0)\rangle^*\ , \tag{32b}$$

where

$$\frac{1}{T_{2Q}^{\Sigma}}=\frac{1}{T_{2Q}^{12,12}}+\frac{1}{T_{2Q}^{12,34}}\ .$$

The magnetization $M\pm(\omega)=N\gamma_I\hbar\langle I\pm\rangle(\omega)$ can be expressed as

$$\langle I_\pm\rangle(\omega)=\sqrt{3}(\langle I_\pm^{12}\rangle+\langle I_\pm^{34}\rangle)(\omega)+2\langle I_\pm^{23}\rangle(\omega)\ , \tag{33a}$$

where $\langle I\pm\rangle(\omega)$ is obtained from $\langle I\pm\rangle^*(\omega)$ by the convolution

$$\langle I_\pm^{ab}\rangle(\omega)=\langle I_\pm^{ab}\rangle^*(\omega)*\delta(\omega\mp\omega_I)\ . \tag{33b}$$

c. Discussion. We have displayed in Figs. 2 and 3 the main observables for a pure quadrupolar relaxation process. Figure 2(a) shows the temperature variation of the spin-spin relaxation rates (Table V) and of the second-order dynamical shifts [Eq. (31)], even when $1/\omega_0\le\tau_c\le 1/H_Q$. There are two interesting features in this figure.

(i) One notes an opposite variation in the low temperature range for the two observable rates labeled "1" and "2". The paradoxical narrowing of the central transition 2-3 when the temperature decreases comes from the nonexistence of the adiabatic part in the T_2 process (see Table V). This is characteristic of the quadrupolar relaxation of a half-integer spin ($I>\frac{1}{2}$) when the perturbation conserves the same value at each time on the two

TABLE V. Elements of spin-spin relaxation rates for the quadrupolar case.

$$\frac{1}{T_{2Q}^{cd,ef}}=3C_Q^2[aJ_0(0)+bJ_1(\omega_I)+cJ_2(2\omega_I)]$$

cd,ef	a	b	c
12,12	1	1	1
12,34	0	0	−1
23,23	0	1	1
34,12=12,34			
34,34=12,12			

central states (e.g., 2 and 3 for $I=\frac{3}{2}$). It results, when the temperature decreases, a sufficiently important narrowing of the central line (2-3) and a broadening of the two other lines (1-2 and 3-4); so only the central line (2-3) is observed [Fig. 2(d)].

(ii) One observes also some temperature ranges where the second-order dynamical shifts ω_Q are of the same order of magnitude and even very much greater than the linewidth. It results important differential shifts ($\omega_Q^{12}=\omega_Q^{34}\neq\omega_Q^{23}$) and linewidths ($1/T_{2Q}^{\Sigma}\neq 1/T_{2Q}^{23,23}$) on the line (2-3) and (1-2 and 3-4) which are really observable when $\tau_c \geq 1/\omega_0$ [Figs. 2(b)–2(d)]. This shows that, even without static quadrupolar splitting, there exists an inherent dissymmetric structure in the line [Fig. 2(c)] which gives supplementary information on the dynamics of the system. There are some recent experiments which use these effects to study the ionic motion in solids.[21]

Figure 3(a) shows the temperature variation of the spin-lattice relaxation rates [Eq. (28)] for the three eigenstates. Figures 3(b)–3(d) show the time dependences of the relative deviation of the longitudinal magnetization at three temperatures for the observable states given in Eqs. (26) and (27). As explained in Fig. 1 and above, only the T_{1Q}^{A} and T_{1Q}^{B} relaxation times [Eq. (28)] can be measured from a saturation or inversion preparation of the longitudinal magnetization.

Since the time evolution of the longitudinal magnetization is obtained through the transverse magnetization after rf irradiation of the spin system, a question arises: what are the relations between such transverse magnetization after the rf pulses and the longitudinal magnetization before the rf pulses? The answer depends on the temperature range considered. For instance in the high-temperature range, $\tau_c \leq 1/\omega_0$, [Figs. 2(b) and 3(b)], the total longitudinal magnetization I_z is transformed after a $\pi/2$ pulse in the total transverse magnetization I_y. In consequence, the vectorial image for the spin operators is still valid and I_y gives complete information about the time evolution of I_z. The relevant curve in Fig. 3(b) is then associated to I_z. In the temperature range $1/\omega_0 \leq \tau_c \leq 1/H_Q$, Figs. 2(c) and 2(d) show that the major part of the signal comes from $\langle I_y^{23}\rangle$. Since

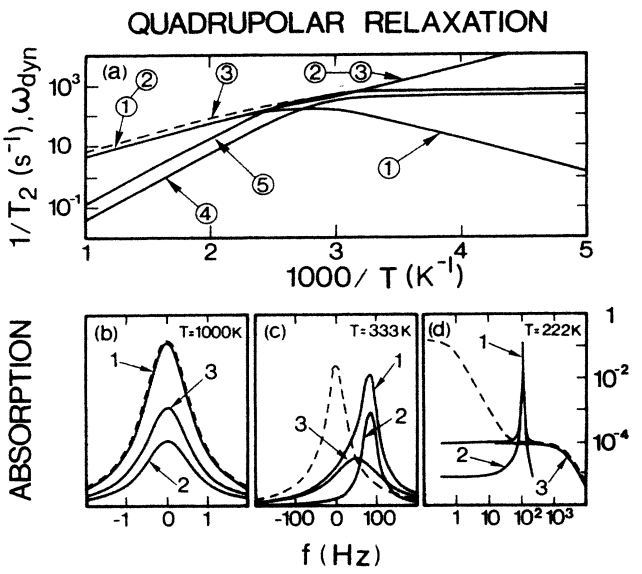

FIG. 2. (a) Semilogarithmic plots of the calculated variation of the spin-spin relaxation rate $1/T_2$ and second-order dynamical shifts ω_{dyn} (both in rad/sec) vs 1000/T(K) for a pure quadrupolar relaxation. The indices 1–3 stand for the eigenstates of the quadrupolar relaxation $I_+^{23}(1), I_+^{12}+I_+^{34}(2)$, and $I_+^{12}-I_+^{34}(3)$, respectively. The dotted lines correspond to the unobservable eigenstates referred to in the text. The indices 4,5 stand for the ω_{dyn}:$\omega^{12}=\omega^{34}(4)$ and $\omega^{23}(5)$, respectively. All these quantities have been calculated with the expression given in Table V and Eq. (31) in using a quadrupolar fluctuation amplitude of 3.5×10^5 rad/sec. (b)–(d) Absorption signals (in arbitrary units) calculated from Eqs. (32) for three temperatures $T=1000$ K (b), 333 K (c), 222 K (d). This illustrates the relative importance of the ω_{dyn} and of the linewidths for the 23 and 12,34 transitions. In each case we have represented the absorption signal with (continuous line) or without (dotted line) ω_{dyn}. The indices 1–3 stand for $\langle I_y\rangle$ (1), $2\langle I_y^{23}\rangle(2)$, and $\sqrt{3}(\langle I_y^{12}+I_y^{34}\rangle)$ (3), respectively. We use linear scales in (b) and (c) and logarithmic scales in (d).

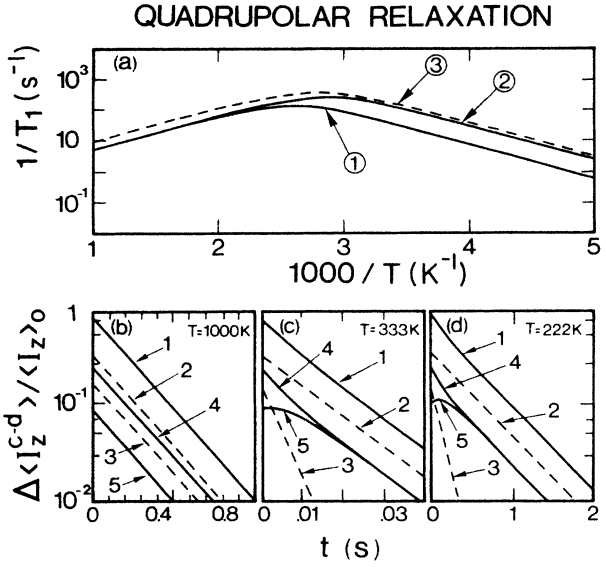

FIG. 3. (a) Semilogarithmic plots of the calculated variation of the spin-lattice relaxation rate $1/T_1$ (in rad/sec) vs 1000/T(K) for a pure quadrupolar relaxation. The indices 1–3 stand for the three eigenstates of the quadrupolar relaxation $\langle I_z^{14}+I_z^{23}\rangle$ (1), $\langle I_z^{14}-I_z^{23}\rangle$ (2), and $\langle I_z^{12}-I_z^{34}\rangle$ (3). The dotted line corresponds to the unobservable eigenstate referred to in the text. All these quantities have been calculated with the expression given in Table IV and Eq. (28) in using a quadrupolar fluctuation amplitude of 3.5×10^5 rad/sec. (b)–(d) Semilogarithmic plots of the time dependences of the relative deviation from equilibrium value, M_0, of the component $\langle I_z^{cd}\rangle$ of the magnetization for three temperatures $T=1000$ K (b), 333 K (c), 222 K (d). In each case we have represented such deviations for the five following states labeled with the indices (1-5) as $\langle I_z\rangle$ (1), $\langle I_z^{14}+I_z^{23}\rangle$ (2), $\langle I_z^{14}-I_z^{23}\rangle$ (3), $\langle I_z^{14}\rangle$ (4) and $\langle I_z^{23}\rangle$ (5), respectively. Here the points correspond to the eigenstates labeled (2) and (3) and the continuous lines to the effectively measured relative deviations as discussed in the text. All the quantities have been calculated from the solution of Eq. (26).

the behavior of $\langle I_y^{23}\rangle$ after rf associates linearly the terms $\langle I_z^{14}(0)\rangle$ and $\langle I_z^{23}(0)\rangle$ before rf, the time dependence of the effectively measured longitudinal magnetization will be a linear combination of the z components in the 14,23 subset. It is interesting to see in Figs. 3(c) and 3(d) that each of these z components follows a different time behavior. The components $\langle I_z^{14}\rangle \pm \langle I_z^{23}\rangle$ decay exponentially because they are two eigenstates for the quadrupolar relaxation. On the contrary $\langle I_z^{14}\rangle$ and $\langle I_z^{23}\rangle$ present a nonexponential time behavior. For $\langle I_z^{23}\rangle$ such time behavior is due to a cross polarization phenomenon between the 1-4 and 2-3 states. This has been observed previously in Li_3N.[27] We will discuss this behavior in the presence of quadrupolar static interaction in Sec. IV.

2. *Dipolar relaxation for like spins*

We consider successively the dipolar relaxation of an ensemble of like (I-I) and unlike (IS) nuclear spins with $I=\frac{3}{2}$ whatever the S value is. The I contribution will be developed on the same basis operators as the one used in the quadrupolar case. This will be useful when considering the superposition of dipolar and quadrupolar relaxations. Let us consider first the modulation of the dipolar interaction ($\Lambda = D_{II}$) between like spins. This means that

$$H_0 = H_Z = \omega_I (I_Z + I'_Z) , \tag{34a}$$

$$H_1(t) = H_{D_{II}}(t) . \tag{34b}$$

According to Eq. (9b) in which $l=2$, the modulation of the dipolar interaction can be written for a two-spin system as

$$H_{D_{II}}(t) = C_D \sum_{m=-2}^{+2} [F_m(t)]^* A_m , \tag{35}$$

where $C_D = -2\gamma_I^2 \hbar$. An elementary transformation in the unique principal axis $\mathbf{r}_{II'}$ joining the two spins, gives for F_m

$$F_m = D^{(2)}_{0m}(0, -\theta, -\phi)\mathcal{T}_0 , \tag{36a}$$

where

$$\mathcal{T}_0 = \sqrt{3/2}\,\delta_D, \quad \mathcal{T}_{\pm 1} = \mathcal{T}_{\pm 2} = 0 , \tag{36b}$$

with

$$\delta_D \equiv 1/(r_{II'})^3 . \tag{36c}$$

Then the A components can be written as

$$A_0 = \frac{1}{\sqrt{6}}(3I_z I_{z'} - \mathbf{I}\cdot\mathbf{I}') , \tag{37a}$$

$$A_{\pm 1} = \mp \tfrac{1}{2}(I_z I'_{\pm} + I_{\pm} I'_z) , \tag{37b}$$

$$A_{\pm 2} = \tfrac{1}{2} I_{\pm} I'_{\pm} . \tag{37c}$$

The spin operators A_m are written in Eqs. (37) as a direct product of two operators acting on subspaces associated to the I and I' degrees of freedom. By the same way the total spin density matrix is defined as $\sigma = \sigma_I \otimes \sigma_{I'}$.

TABLE VI. Elements of spin-lattice relaxation rates for the dipolar case with like spins.

$$\frac{1}{T_{1D_{II}}^{cd,ef}} = \tfrac{1}{3} I(I+1) C_D^2 [a J_0(0) + b J_1(\omega_I) + c J_2(2\omega_I)]$$

cd,ef	a	b	c
14,14	$\frac{1}{10}$	$\frac{3}{4}$	$\frac{12}{5}$
14,23	$-\frac{3}{10}$	$-\frac{3}{4}$	$-\frac{6}{5}$
23,14=14,23			
23,23	$\frac{9}{10}$	$\frac{11}{4}$	$\frac{28}{5}$
12,34	$\frac{1}{2}$	$\frac{3}{2}$	3

In the interaction representation Eq. (10) reduces to

$$e^{iH_0 t} A_m e^{-iH_0 t} = A_m e^{im\omega_I t} . \tag{38}$$

a. Spin-lattice relaxation. Following the same procedure used for the quadrupolar case but with the commutators obtained similarly to those of Appendix A, one has the following longitudinal kinetic equations:

$$\frac{d}{dt}\begin{pmatrix} \langle I_z^{14}\rangle^* \\ \langle I_z^{23}\rangle^* \\ (\langle I_z^{12}\rangle - \langle I_z^{34}\rangle)^* \end{pmatrix} = -\left[\frac{1}{\mathbf{T}_{1D_{II}}}\right] \begin{pmatrix} \Delta\langle I_z^{14}\rangle^* \\ \Delta\langle I_z^{23}\rangle^* \\ \Delta(\langle I_z^{12}\rangle - \langle I_z^{34}\rangle)^* \end{pmatrix} , \tag{39}$$

where the spin lattice relaxation rates are given in Table VI where the other elements are equal to zero. One finds three eigenstates for the dipolar relaxation matrix: $\langle I_z\rangle = 3\langle I_z^{14}\rangle^* + \langle I_z^{23}\rangle^*$, $\langle I_z^{14}\rangle^* - 3\langle I_z^{23}\rangle^*$, and $\langle I_z^{12}\rangle^* - \langle I_z^{34}\rangle^*$ associated respectively to the three relaxation rates:

$$\begin{aligned} \frac{1}{T_{1D}^A} &= \tfrac{1}{3} I(I+1) C_D^2 [\tfrac{1}{2} J_1(\omega_I) + 2J_2(2\omega_I)] , \\ \frac{1}{T_{1D}^B} &= \tfrac{1}{3} I(I+1) C_D^2 [J_0(0) + 3J_1(\omega_I) + 6J_2(2\omega_I)] , \\ \frac{1}{T_{1D}^C} &= \tfrac{1}{3} I(I+1) C_D^2 [\tfrac{1}{2} J_0(0) + \tfrac{3}{2} J_1(\omega_1) + 3J_2(2\omega_I)] . \end{aligned} \tag{40}$$

Of course, the first rate $1/T_{1D}^A$ is the well known spin relaxation rate $1/T_{1D}$ given in Ref. 6(a). For the other two modes of relaxation, one sees in Fig. 1 that the deviations Δ from equilibrium of the population differences between the levels involved in their associated eigenstates are zero whether for saturation or inversion experiments. In consequence only the first rate $1/T_{1D}^A$ drives the dipolar relaxation process for like spins.

b. Spin-spin relaxation. Using the commutators obtained similarly to those of Appendix A, one has the following kinetic equations for the transverse relaxation

$$\frac{d}{dt}\begin{bmatrix}\langle I_{\pm}^{12}\rangle^* \\ \langle I_{\pm}^{23}\rangle^* \\ \langle I_{\pm}^{34}\rangle^*\end{bmatrix} = -\left[\frac{1}{\mathbf{T}_{2D_{II}}} \mp i\omega_{D_{II}}\mathbf{1}\right]\begin{bmatrix}\langle I_{\pm}^{12}\rangle^* \\ \langle I_{\pm}^{23}\rangle^* \\ \langle I_{\pm}^{34}\rangle^*\end{bmatrix} \quad (41)$$

where the dipolar dynamical shift is given by

$$\omega_{D_{II}} = \tfrac{1}{3}I(I+1)C_D^2[\tfrac{1}{2}K_1(\omega_I)+K_2(2\omega_I)] \; . \quad (42)$$

and the spin-spin relation rates are given in Table VII.

The solution of Eq. (41), in the frequency domain, is obtained after some algebraic manipulations which give

$$\langle I_{\pm}\rangle(\omega) = \frac{T_{2D} - i(\omega \mp \omega_{D_{II}})(T_{2D})^2}{1+[(\omega \mp \omega_{D_{II}})(T_{2D})]^2}\langle I_{\pm}(0)\rangle * \delta(\omega \mp \omega_I) \; , \quad (43)$$

where T_{2D} is the well-known transverse relaxation time defined as

$$\frac{1}{T_{2D}} = \tfrac{1}{3}I(I+1)C_D^2[\tfrac{3}{4}J_0(0)+\tfrac{5}{4}J_1(\omega_I)+\tfrac{1}{2}J_2(2\omega_I)] \; . \quad (44)$$

Equation (43) shows that the second-order dynamic shift and the homogeneous linewidth do not depend on the transitions. So the dipolar modulation for like spins does not split the line but shifts it.

c. Discussion. We have displayed in Figs. 4(a) and 4(b) the temperature variation of the spin-lattice and spin-spin relaxation rates for a pure dipolar relaxation process. As shown above, one has only one T_{1D} and one T_{2D} driving the dipolar relaxation for the direction I_z and $\sqrt{3}(I_{\pm}^{12}+I_{\pm}^{34})+2I_{\pm}^{23}$ (i.e., $I_{\pm}$), respectively. The other directions of relaxation will be useful in Sec. III B to study the superposition of a dipolar and quadrupolar relaxation processes. In Fig. 4(b) one sees that the second-order dynamical shift ω_{DII} stays always much smaller than the homogeneous linewidth T_{2D}^{-1}, thus inducing an insignificant lineshift.

3. *Dipolar relaxation for unlike spins*

In this section we consider the modulation of the dipolar interaction ($\Lambda = D_{IS}$) between unlike spins $I = \frac{3}{2}$

TABLE VII. Elements of spin-spin relaxation rates for the dipolar case with like spins.

$$\frac{1}{T_{2D_{II}}^{cd,ef}} = \tfrac{1}{3}I(I+1)C_D^2[aJ_0(0)+bJ_1(\omega_I)+cJ_2(2\omega_I)]$$

cd,ef	a	b	c
12,12	$\frac{17}{20}$	$\frac{19}{10}$	$\frac{5}{2}$
12,23	$-\sqrt{3}/10$	$-2\sqrt{3}/5$	$-\sqrt{3}$
12,34	$\frac{1}{10}$	$\frac{3}{20}$	0
23,12=12,23=			
23,34=34,23			
23,23	$\frac{21}{20}$	$\frac{49}{20}$	$\frac{7}{2}$
34,12=12,34			
34,34=12,12			

TABLE VIII. Transition frequencies ω_m^p and spin operators $\mathbf{A}_m^p$ for unlike spins.

$m=0$	$A_0^0 = \frac{2}{\sqrt{6}}I_zS_z$,	$\omega_0^0 = 0$
	$A_0^{\pm 1} = -\frac{1}{2\sqrt{6}}I_{\pm}S_{\mp}$,	$\omega_0^{\pm 1} = \pm(\omega_I - \omega_S)$
$m=\pm 1$	$A_{\pm 1}^1 = \mp\frac{1}{2}I_{\pm}S_z$,	$\omega_{\pm 1}^1 = \pm\omega_I$
	$A_{\pm 1}^2 = \frac{1}{2}I_zS_{\pm}$,	$\omega_{\pm 1}^2 = \pm\omega_S$
$m=\pm 2$	$A_{\pm 2}^1 = \frac{1}{2}I_{\pm}S_{\pm}$,	$\omega_{\pm 2}^1 = \pm(\omega_I + \omega_S)$

whatever the S value is. This means that

$$H_0 = H_Z = \omega_I I_z + \omega_S S_z \; , \quad (45a)$$

$$H_1(t) = H_{DIS}(t) \; . \quad (45b)$$

The expression of $H_{DIS}(t)$ is obtained by substituting in Eqs. (36)–(38) I' by S. Using Eq. (10), one obtains the transition frequencies ω_m^p and spin operators A_m^p given in Table VIII.

a. Spin-lattice relaxation. Here one obtains the following longitudinal kinetic equations

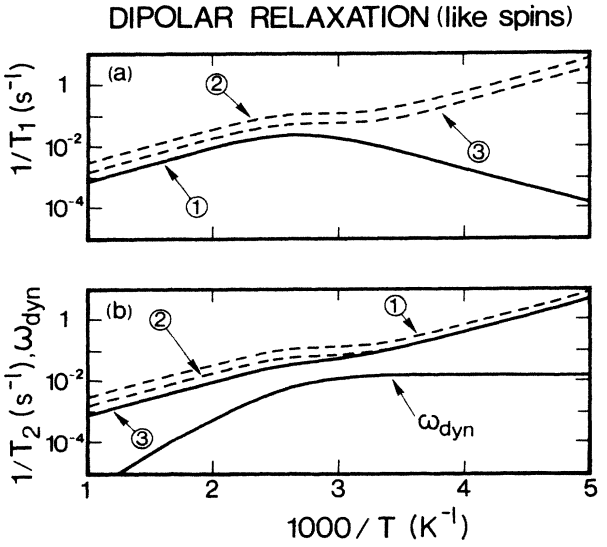

FIG. 4. (a) Semilogarithmic plots of the calculated variation of the spin-lattice relaxation rate $1/T_1$ (in rad/sec) vs 1000/T(K) for a pure dipolar (like spins $I = \frac{3}{2}$) relaxation. The indices 1–3 stand for the eigenstates of the dipolar relaxation $\langle I_z\rangle$ (1) (continuous line) $\langle I_z^{14}-3I_z^{23}\rangle$ (2), and $\langle I_z^{12}-I_z^{34}\rangle$ (3) (dotted lines), respectively. The different $1/T_1$ have been calculated with Table VI and Eq. (40) in using a dipolar fluctuation amplitude of 6.9×10^3 rad/sec. (b) Semilogarithmic plots of the calculated variation of the spin-spin relaxation rate $1/T_2$ and dynamical shifts ω_{dyn} (both in rad/sec) vs 1000/T(K) for a pure dipolar (like spins) relaxation. The indices 1–3 stand for the unobservable states $\sqrt{3}(I_+^{12}+I_+^{34})-3I_+^{23}$ (1) and $3(I_+^{12}-I_+^{34})$ (2) in dotted lines, and the observable one I_+ (3) in continuous line. The different $1/T_2$ have been calculated with Table VII in using a dipolar fluctuation amplitude of 6.9×10^3 rad/sec. The single ω_{dyn} has been calculated from Eq. (42).

TABLE IX. Spin-lattice relaxation rates for the dipolar case with unlike spins.

$$\frac{1}{T_i^{XY}}=\frac{Z(Z+1)}{3}C_{D_{IS}}^2[aJ_0(0)+bJ_0(\omega_I-\omega_S)+cJ_1(\omega_I)+dJ_1(\omega_S)+eJ_2(\omega_I+\omega_S)]$$

i^{XY}	Z	a	b	c	d	e
1^{II}	S	0	$\frac{1}{6}$	$\frac{1}{2}$	0	1
1^{IS}	I	0	$-\frac{1}{6}$	0	0	1
1^{SS}	I	0	$\frac{1}{6}$	0	$\frac{1}{2}$	1
1^{SI}	S	0	$-\frac{1}{6}$	0	0	1
2^{I}	S	$\frac{1}{3}$	$\frac{1}{12}$	$\frac{1}{4}$	$\frac{1}{2}$	$\frac{1}{2}$
2^{S}	I	$\frac{1}{3}$	$\frac{1}{12}$	$\frac{1}{2}$	$\frac{1}{4}$	$\frac{1}{2}$

$$\frac{d}{dt}\begin{bmatrix}\langle I_z^{14}\rangle^* \\ \langle I_z^{23}\rangle^* \\ \langle S_z\rangle^* \\ \langle I_z^{12}\rangle^*-\langle I_z^{34}\rangle^*\end{bmatrix}=-\begin{bmatrix}\frac{3}{2}\frac{1}{T_1^{II}} & -\frac{3}{2}\frac{1}{T_1^{II}} & \frac{3}{10}\frac{1}{T_1^{IS}} & 0 \\ -\frac{3}{2}\frac{1}{T_1^{II}} & \frac{11}{2}\frac{1}{T_1^{II}} & \frac{1}{10}\frac{1}{T_1^{IS}} & 0 \\ 3\frac{1}{T_1^{SI}} & \frac{1}{T_1^{SI}} & \frac{1}{T_1^{SS}} & 0 \\ 0 & 0 & 0 & \frac{3}{T_1^{II}}\end{bmatrix}\begin{bmatrix}\Delta\langle I_z^{14}\rangle^* \\ \Delta\langle I_z^{23}\rangle^* \\ \Delta\langle S_z\rangle^* \\ \Delta(\langle I_z^{12}\rangle^*-\langle I_z^{34}\rangle^*)\end{bmatrix} \tag{46}$$

where the spin-lattice relaxation rates are given in Table IX. In this Table $C_{DIS}=-2\gamma_I\gamma_S\hbar$ and the notations $1/T_1^{II},\ldots,$ are similar to the one used by Abragam.[6(a)]

Introducing the following terms: $\langle I_z\rangle=3\langle I_z^{14}\rangle+\langle I_z^{23}\rangle,\langle S_z\rangle$, and the other ones given in Eq. (47), Eq. (46) becomes

$$\frac{d}{dt}\begin{bmatrix}\langle I_z\rangle^* \\ \langle S_z\rangle^* \\ \langle I_z^{12}\rangle^*-\langle I_z^{34}\rangle^* \\ \langle I_z^{14}\rangle^*-3\langle I_z^{23}\rangle^*\end{bmatrix}=-\begin{bmatrix}\frac{1}{T_1^{II}} & \frac{1}{T_1^{IS}} & 0 & 0 \\ \frac{1}{T_1^{SI}} & \frac{1}{T_1^{SS}} & 0 & 0 \\ 0 & 0 & \frac{3}{T_1^{II}} & 0 \\ 0 & 0 & 0 & \frac{6}{T_1^{II}}\end{bmatrix}\begin{bmatrix}\Delta\langle I_z\rangle^* \\ \Delta\langle S_z\rangle^* \\ \Delta(\langle I_z^{12}\rangle^*-\langle I_z^{34}\rangle^*) \\ \Delta(\langle I_z^{14}\rangle^*-3\langle I_z^{23}\rangle^*)\end{bmatrix}. \tag{47}$$

Of course in the $\langle I_z\rangle,\langle S_z\rangle$ subspace, one finds again the well-known coupled kinetic equations (6a) which describe the cross-relaxation phenomenon between the only two observable magnetizations. On the other two directions, one notes that the eigenstates for the dipolar (unlike) cases are exactly the same as the one for the dipolar (like) cases.

b. Spin-spin relaxation. Using the same method, one has the following kinetic equations for the transverse relaxation

$$\frac{d}{dt}\begin{bmatrix}\langle I_\pm^{12}\rangle \\ \langle I_\pm^{23}\rangle \\ \langle I_\pm^{34}\rangle\end{bmatrix}=-\left[\frac{1}{\mathbf{T}_{2D_{IS}}}\mp i\omega_{D_{IS}}\mathbf{1}\right]\begin{bmatrix}\langle I_\pm^{12}\rangle \\ \langle I_\pm^{23}\rangle \\ \langle I_\pm^{34}\rangle\end{bmatrix}, \tag{48a}$$

$$\frac{d}{dt}\langle S_+\rangle^*=-\left[\frac{1}{\mathbf{T}_2^S}\mp i\omega_{D_{SI}}\mathbf{1}\right]\langle S_+\rangle^*, \tag{48b}$$

where the transverse relaxation matrix $[1/T_{2DIS}]$ and the dynamical shifts ω_{DIS} and ω_{DSI} are given by

$$\left[\frac{1}{\mathbf{T}_{2D_{IS}}}\right]=\begin{bmatrix}\frac{1}{T_2^I}+\frac{2}{T_1^{II}} & -\frac{\sqrt{3}}{T_1^{II}} & 0 \\ -\frac{\sqrt{3}}{T_1^{II}} & \frac{1}{T_2^I}+\frac{3}{T_1^{II}} & -\frac{\sqrt{3}}{T_1^{II}} \\ 0 & -\frac{\sqrt{3}}{T_1^{II}} & \frac{1}{T_2^I}+\frac{2}{T_1^{II}}\end{bmatrix}, \tag{49}$$

$$\omega_{D_{IS}}=\tfrac{1}{3}S(S+1)[\tfrac{1}{6}K_0(\omega_I-\omega_S)+\tfrac{1}{2}K_1(\omega_I)+K_2(\omega_I+\omega_S)], \tag{50a}$$

$$\omega_{D_{SI}}=\tfrac{1}{3}I(I+1)[\tfrac{1}{6}K_0(\omega_S-\omega_I)+\tfrac{1}{2}K_1(\omega_S)+K_2(\omega_I+\omega_S)]. \tag{50b}$$

The solution of Eq. (48a) in the frequency domain gives for $\langle I\pm\rangle(\omega)$

$$\langle I_{\pm}\rangle(\omega)=\langle I_{\pm}(0)\rangle \left[\frac{T_2^I \mp(\omega-\omega_{D_{IS}})(T_2^I)^2}{1+[(\omega-\omega_{D_{IS}})(T_2^I)]^2}\right] * \delta(\omega\pm\omega_I) , \tag{51}$$

and the like expression for $\langle S_{\pm}\rangle(\omega)$ by interchanging I and S. Equation (51) shows that the second-order dynamic shift and the homogeneous linewidth do not depend on the transitions. So the dipolar modulation whether for like or unlike spins does not split the line but shifts it. As usual the spin-spin relaxation process are decoupled in I and S.

c. Discussion. We have plotted in Figs. 5(a)–5(c) the temperature variation of the spin-lattice [Fig. 5(a)] and spin-spin [Fig. 5(b) and 5(c)] relaxation rates for a dipolar relaxation process (unlike spins).

As explained above there are only two observable spin-lattice relaxation rates in this case [labeled I_z and S_z in Fig. 5(a)]. These two rates are the eigenvalues of the coupled kinetic equations in the I_z,S_z subspace. Physically they represent the trend to equilibrium of two coupled reservoirs associated to the I and S spin systems connected with a lattice. One of these rates [lower continuous line in Fig. 5(a)] corresponds to the direct relaxation of either I or S systems to the lattice. The other one [upper continuous line in Fig. 5(a)] corresponds to both the direct or the indirect relaxation (via the cross relaxation phenomenon). One sees on this figure that their temperature variations are different. At low temperature the cross relaxation dominates largely over the direct relaxation because the cutoff of the spectral density corresponds to characteristic frequencies $\omega_I-\omega_S$ of the spin system. This corresponds to the flip-flop transitions associated to the $J_0(\omega_I-\omega_S)$ contribution which enhances the T_1^{-1} by a factor $\omega_I/(\omega_I-\omega_S)$ at this temperature. Due to the nonequivalence of the I and S spins these transitions are nonresonant and the presence of the lattice is necessary to conserve the total energy in the relaxation process. At high temperature the spectral density spreads over a wider range of frequency with a cutoff either for ω_I or ω_S. The $J_0(\omega_I-\omega_S)$, $J_1(\omega_I)$, $J_1(\omega_S)$, and $J_2(\omega_I+\omega_S)$ contributions are of the same order of magnitude and the two mechanisms of relaxation present an identical temperature variation.

Since the spin-spin relaxation is decoupled for I and S spins, we have decoupled their temperature dependences in two different figures [Figs. 5(b) and 5(c)]. As in the dipolarlike case, the dynamical shifts stay always much smaller than the homogeneous linewidths, thus producing insignificant line shifts. However, one notes for the I spin [inset of Fig. 5(b)] a change of sign of the dynamical shift at low temperature [$\tau_c\sim 1/(\omega_I-\omega_S)$]. This is due to the $K_0(\omega_I-\omega_S)$ contribution which dominates at this temperature.

B. Multiple sources of relaxation

The formalism presented above allows to define easily the total matrix of relaxation, for a mixing of different fluctuations, by using the individual matrices associated to each of these fluctuations. In this section we consider explicitly the cases of a mixing of quadrupolar and dipolar (like and unlike) fluctuations which mostly occur in real materials.

1. Mixing of quadrupolar and dipolar (like spins) relaxations

In order to obtain the kinetic equations for the longitudinal and transverse magnetizations, we take into ac-

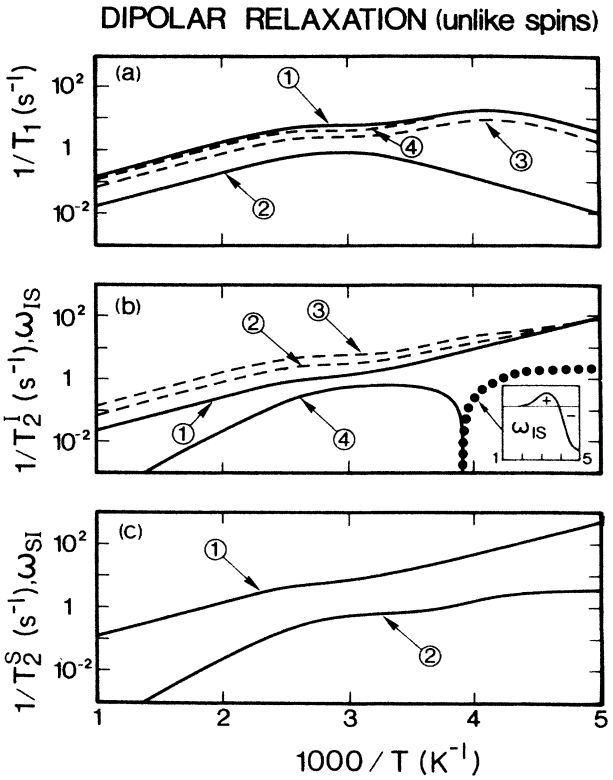

FIG. 5. (a) Semilogarithmic plots of the calculated variation of the spin-lattice relaxation rate $1/T_1$ (in rad/sec) vs 1000T/(K) for a pure dipolar (unlike spins $I=\frac{3}{2}$, here $S=\frac{1}{2}$) relaxation. The indices 1–4 stand for the eigenstates of the dipolar relaxation $\langle I_z\rangle$ (1), $\langle S_z\rangle$ (2) (continuous lines), $\langle I_z^{12}-I_z^{34}\rangle$ (3), and $\langle I_z^{14}-3I_z^{23}\rangle$ (4) (dotted lines), respectively. The different $1/T_1$ have been calculated with Table IX in using a dipolar fluctuation amplitude of 6.9×10^3 rad/sec for Λ_{IS} where we have chosen the particular case: Lithium (spin I) and phosphorus (spin S). (b) Semilogarithmic plots of the calculated variation of the spin-spin relaxation rate $1/T_2^I$ and dynamical shifts $\omega_{\rm dyn}$ (both in rad/sec) vs 1000/T(K) for a pure dipolar (unlike spins $I=\frac{3}{2}$, here $S=\frac{1}{2}$) relaxation. The indices 1–3 stand for the eigenstates of the dipolar relaxation for $[1/\mathbf{T}_2]$: $\sqrt{3}\langle I_+^{12}+I_+^{34}\rangle+2\langle I_+^{23}\rangle$ (1) (continuous line), $\sqrt{3}\langle I_+^{12}-I_+^{34}\rangle$ (2), and $\sqrt{3}\langle I_+^{12}+I_+^{34}\rangle-3\langle I_+^{23}\rangle$ (3) (dotted lines). The different $1/T_2$ have been calculated from Eq. (49) with the last two lines of Table IX in using a dipolar fluctuation amplitude of 6.9×10^3 rad/sec for Λ_{IS} where we have chosen the particular case: Lithium (spin I) and phosphorus (spin S). The $\omega_{\rm dyn}$ (spin I), labeled by the index (4), has been calculated by Eq. (50a). In insert we give the linear temperature variation of $\omega_{\rm dyn}$. (c) Same legend as (b) but for the spin S, with $\langle S_+\rangle$ as eigenstate for $[1/\mathbf{T}_2^S]$ and $\omega_{\rm dyn}$ given by Eq. (50b).

count the sum of the matrices given in Eq. (26) and Eq. (39) for $[1/T_1]$ and in Eq. (30) and Eq. (41) for $[1/T_2]$ since the results of the calculations have been expressed in the same basis sets.

In Fig. 6, we show the temperature variation of the spin-spin, dynamical shifts [Fig. 6(a)] and spin-lattice [Fig. 6(b)] relaxation rates. The comparison between these figures and those of the pure quadrupolar fluctuations [Figs. 2(a) and 3(a)] shows that in a wide temperature range the quadrupolar fluctuations drive the relaxation process. However when the dipolar adiabatic part is of the same order of magnitude as the quadrupolar lifetimes the dipolar fluctuations modify drastically the temperature behavior of the relaxation rates. For instance at low temperature the linewidth associated to the 2-3 transition becomes mainly due to the adiabatic fluctuations [Fig. 6(a)]. On the contrary the linewidth associated to the 1-2 and 3-4 transitions stays monitored by the quadrupolar fluctuations. In the same low-temperature regime, one of the observable spin-lattice relaxation rates increases and the other decreases with the temperature [Fig. 6(b)]. According to the discussion given in Sec. III A 1 c, we know that the time dependence of the effectively measured longitudinal magnetization is a linear combination of the z components in the 1-4,2-3 subsets and not only a pure $\langle I_z \rangle^*$. In this subspace, the shortest relaxation time is representative of the cross-relaxation assisted by the dipolar flip-flop transitions between the levels and the longest relaxation time reflects the return of the total magnetization to the equilibrium.

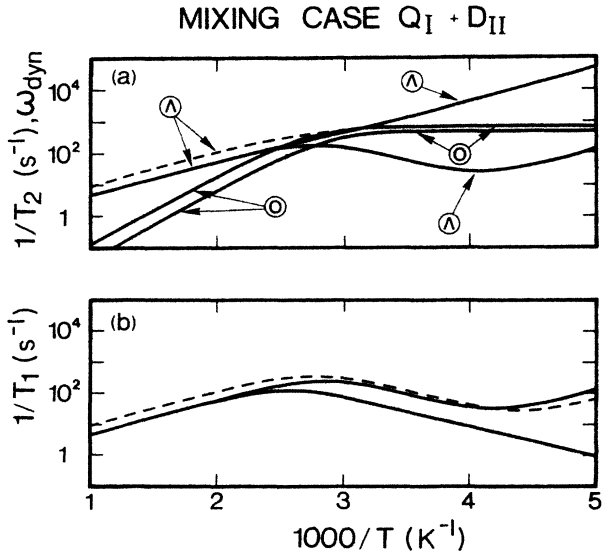

FIG. 6. (a) Semilogarithmic plots of the calculated variation of the spin-spin relaxation rate $1/T_2$ (in rad/sec) vs 1000/T(K) for a mixing of quadrupolar and dipolar (like spins) relaxation. The symbols Λ and O stand for the different $1/T_2$ (see the Sec. III B) and ω_{dyn}, respectively. (b) Semilogarithmic plots of the calculated variation of the spin-lattice relaxation rate $1/T_1$ (in rad/sec) vs 1000/T(K) for a mixing of quadrupolar and dipolar (like spins) relaxation.

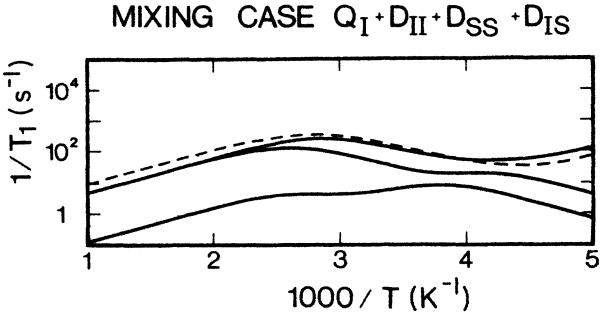

FIG. 7. Semilogarithmic plots of the calculated variation of the spin-lattice relaxation rate $1/T_1$ (in rad/sec) vs 1000/T(K) for mixing of quadrupolar and dipolar (like spins) and dipolar (unlike spins) relaxation (see the text, Sec. III B, for explaining the curves.).

2. *Mixing of quadrupolar, dipolar (like spins) and dipolar (unlike spins) relaxations*

Finally we consider the complete mixing case which takes into account all the individual fluctuations described above (noted $Q_I + D_{II} + D_{IS} + D_{SS}$). In Fig. 7, we show the temperature variation of the three observable spin-lattice relaxation rates (I and S spins). The similar variation for the spin-spin relaxation rates and dynamical shifts are omitted because of their similarities with the preceding mixing case for the I spin and with the D_{IS} case for the S spins.

There are interesting new feature in this figure. Namely, when we compare the longest longitudinal relaxation time here and in the pure D_{IS} case [Fig. 5(a)], one notes a practically temperature independence of this rate over a large temperature range (200 K for the correlation function used here). For the shortest longitudinal relaxation rate, the temperature variation is quadrupolarlike with a noticable difference at low temperature due to the dipolarlike flip-flop fluctuations. The intermediate relaxation rate is monitored by the quadrupolar fluctuations up to a correlation time $\tau_c \sim 1/(\omega_I - \omega_S)$ where the dipolar (unlike) fluctuations dominate again. This is exactly what happened, at low temperature, in Fig. 5(a).

What is particularly significant here is the *different maxima* in the temperature variation of the observable spin-lattice relaxation rates obtained with *a single exponential correlation function.* As proved in this paper, by choosing on purpose the same monoexponential correlation function for all the fluctuations, this is due to the repartition in the spectral domain of the characteristic frequencies of the transitions created by the various kinds of fluctuations. This shows the importance of a correct treatment of the quantum part of the relaxation process before trying to interpret the dynamics from the data.

IV. APPLICATION TO QUADRUPOLAR AND DIPOLAR RELAXATIONS INCLUDING A RESIDUAL TIME AVERAGED INTERACTION

In this section we include, in the relaxation, the presence of a static or residual time averaged quadrupolar

interaction $\bar{H}_Q$. For example, in superionic conductors, this latter interaction may come when the nuclear spin tensorial interactions are not averaged to zero by the local or long range ionic motions.[17,18] This induces some modifications in the relaxation results, namely a splitting of the Zeeman frequencies and a slow oscillating time-dependent term in the spin-spin relaxation rate according to Eq. (18). We discuss below the effects of such residual interaction on the spin-lattice and spin-spin rates in the different cases considered in Sec. III.

A. Discussion

Here the static Hamiltonian H_0 and the time-dependent perturbation $H_1(t)$ are given, respectively by

$$H_0 = H_Z + \bar{H}_Q \ ; \tag{52a}$$

$$H_1(t) = H_Q(t), \text{ or } H_{DII}(t), \text{ or } H_{DIS}(t) \ , \tag{52b}$$

or mixing of these perturbations, where H_Z and $\bar{H}_Q(t)$ are defined in Eqs. (20a) or (45a) and (21), (34b), and (45b), respectively. We restrict $\bar{H}_Q$ to its first-order approximation, thus neglecting again the fast oscillating terms in the rotating frame. This gives

$$\bar{H}_Q = \Omega_Q (I_z^{12} - I_z^{34}) \tag{53a}$$

with

$$\Omega_Q = \tfrac{3}{2} C_Q \delta_Q \overline{\{(3\cos^2\theta - 1) + \eta_Q \sin^2\theta \cos 2\alpha\}} \ , \tag{53b}$$

where C_Q, δ_Q, η_Q, θ, and α are defined in Sec. III A 1 and the overbar stands for the time average.

Using the same procedure as in Sec. III but with H_0 given in Eq. (52a) leads, after straightforward calculations, to the spin-lattice and spin-spin relaxation rates given in the tables of Appendix B.

In Fig. 8, we show the temperature variation of the spin-lattice relaxation rates for the different fluctuations. The comparison with the case of $\Omega_Q = 0$ shows the disappearance of the dotted lines when $\Omega_Q \neq 0$. This means that all the rates defined in the tables could be theoretically observable. This comes from the coupling of all the components of the longitudinal magnetization by the relaxation process. One should note that the coupling terms, for any fluctuations, are composed by a superposition of differences of spectral densities like $J_{\Lambda m}(m\omega_I + \Omega_Q) - J_{\Lambda m}(m\omega_I - \Omega_Q)$. These differences are close to zero in case of monoexponential correlation functions, thus involving the classical relaxation behavior described above. On the contrary these differences can be far from zero when the individual spectral densities vary drastically with the frequency. This occurs when considering properly the local[28] and/or the low dimensional motions[2,23,25] which produce a residual time averaged quadrupolar interaction $\Omega_Q \neq 0$. We will see in a following paper such effect on the spin relaxation rates in superionic conductors of low symmetry. Moreover, at low temperature, another difference with the case $\Omega_Q = 0$ comes from the cross relaxation due to the flip-flop dipolar terms. This is particularly evident in the pure dipolar case [Fig. 8(b)] where a second maximum of $1/T_1$

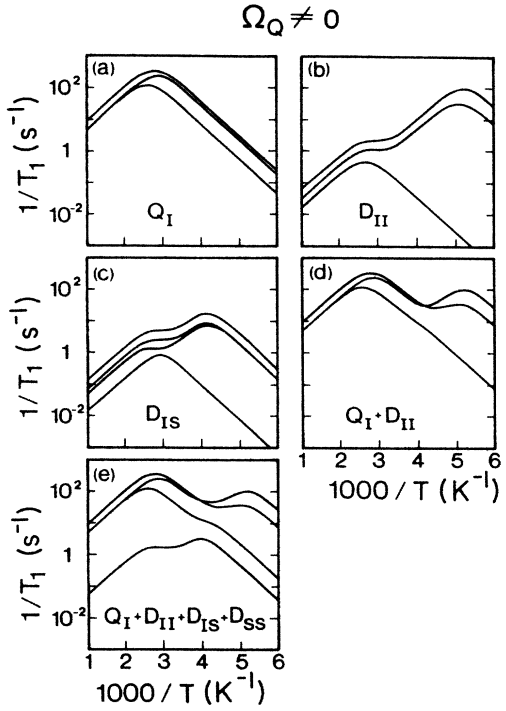

FIG. 8. Semilogarithmic plots of the calculated variations of the spin-lattice relaxation rate $1/T_1$ (in rad/sec) vs 1000/T(K) in presence of a residual time averaged quadrupolar interaction $\Omega_Q = 30$ KHz for various fluctuations: (a) pure quadrupolar; (b) dipolar (like spins); (c) dipolar (unlike spins); (d) mixing of quadrupolar and dipolar (like spins); (e) mixing of quadrupolar and dipolar (like and unlike spins). The corresponding fluctuation amplitudes are the same as in the case $\Omega_Q = 0$, respectively.

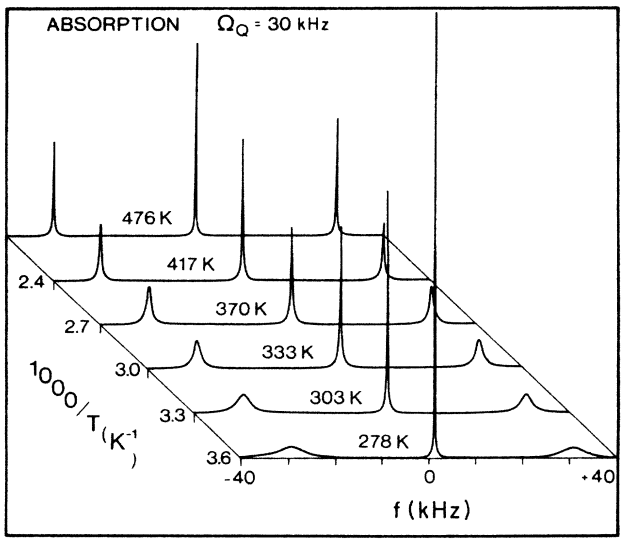

FIG. 9. Absorption signals (in arbitrary units) at six temperatures for a pure quadrupolar relaxation process in presence of a residual time averaged quadrupolar interaction $\Omega_Q = 30$ KHz. The quadrupolar fluctuation amplitude is 1.2×10^6 rad/sec.

occurs in this temperature range when the cutoff time τ_c is about $1/\Omega_Q$. The two orders of magnitude separating these different maxima comes from the ratio ω_I/Ω_Q between the corresponding values of T_1. Concerning the mixing cases shown in Figs. 8(d) and 8(e), the occurrence of different observable maxima with a single exponential correlation function is emphasized by the presence of $\Omega_Q \neq 0$.

In Fig. 9 we have displayed the spectrum at different temperatures for a pure quadrupolar relaxation process in presence of $\Omega_Q \neq 0$. The most interesting feature is the emergence of a well-defined structure observed when the temperature increases. As explained above this comes from the adiabatic terms which dominate the homogeneous linewidth of the satellites while the nonadiabatic terms determined the linewidth of the central line. This theoretical behavior is in very good agreement with the evolution of the ^{7}Li absorption spectra with temperature described in the Fig. 6 of Ref. 17. One notes also at the higher temperature that the ratio between the different lines is different from the well-known 3-4-3 ratio expected for a quadrupolar spectrum. This is due to the evolution of the density matrix during the preparatory pulse which allows to insert the initial value in the calculation of the spectrum. During this pulse a part of the signal goes to some coherences which are not detected by a simple pulse.[29,30]

B. Homogeneous linewidths of the multiquanta spectra

Though the preparation of multiquanta excitation is well described.[16,31] The discussion of the quadrupolar relaxation of such transitions has not been made already. We have then applied our formalism to deal with such a problem and propose in the tables of Appendix B the spin-spin relaxation matrices of the double- and triple-quantum spectra. Following such tables the double-quantum spectrum is composed of two lines whose temperature behavior is similar to that of the satellites in the monoquantum spectrum. On the contrary, the triple-quantum spectra has a temperature behavior similar to the central line of the monoquantum spectra.

V. CONCLUSION

We have used the fictitious spin-$\frac{1}{2}$ operator formalism to describe the nuclear relaxation of spins $I > \frac{1}{2}$ in solids. We found a generalized macroscopic kinetic differential equation for any observable, expanded on a complete basis set of independent fictitious spin-$\frac{1}{2}$ operators, and whose time evolution is expressed in terms of a matrix of relaxation. The interest of such method is to allow a possible treatment of the relaxation whether for single or multiple relaxation processes. In this latter case by simply adding the individual matrix in the corresponding basis subset. Our calculations include formally the treatment of a residual nonaveraged perturbation term which could affect the relaxation when its amplitude is at least of the same order of magnitude as the one inducing the relaxation itself.

We have applied this treatment to the quadrupolar ($I = \frac{3}{2}$) and dipolar relaxation for like spins ($I = \frac{3}{2}$) and unlike spins ($S = \frac{1}{2}$) but also to the mixing case of these two kinds of relaxation. In each case theoretical expressions and diagrams have been given to follow the temperature variation of the spin-spin and spin-lattice relaxation rates. We give also, for the quadrupolar relaxation at three different temperatures, the spectrum and the time evolution of the relative deviation from equilibrium of the longitudinal magnetization.

For quadrupolar relaxation ($I = \frac{3}{2}$) we found an opposite variation, in the low-temperature range, for the two observable spin-spin relaxation rates. The paradoxical narrowing of the central transition when the temperature decreases has been explained by the nonexistence of the adiabatic part in the T_2 process for a half-integer spin ($I > 1/2$). In some temperature range it is shown that the second-order dynamical shifts are of the same order of magnitude and even much greater than the homogeneous linewidths. It results in important temperature dependent differential shifts and linewidths on the central and other lines which could be observable. This predicts that, even without static quadrupolar splitting, there exists an inherent structure in the line. This effect could give supplementary information on the dynamics of the system. Concerning the measurement of the spin-lattice relaxation rate, we have shown that in the high-temperature range, $\tau_c \leq 1/\omega_0$, the vectorial image for the spin operators is still valid and I_y gives a complete information about the time evolution of the total magnetization I_z which is exponentially decreasing. However, in the intermediate temperature range $1/\omega_0 \leq \tau_c \leq 1/H_Q$, the major part of the signal comes from the transverse magnetization associated with the central transition. Here the vectorial image is not any more valid and the longitudinal magnetization presents a pronounced nonexponential time decay.

For dipolar relaxation (unlike spins: i.e., $I = \frac{3}{2}$ and $S = \frac{1}{2}$) an interesting new feature in the temperature variation of the spin-lattice relaxation rates has been evidenced at low temperature. Namely the dominance of the cross relaxation over the direct relaxation which enhances largely the T_1^{-1} by a factor $\omega_I/(\omega_I - \omega_S)$.

We have considered the complete mixing case of quadrupolar and dipolar (like and unlike spins) relaxations. We note a practically temperature independence of the longest longitudinal relaxation time over a very large temperature range. While the temperature variation of the shortest longitudinal relaxation time is practically quadrupolarlike with only a noticeable difference at low temperature due to the dipolar cross relaxation which enhances such rate. It results in different maxima in these temperature dependences which have been explained in terms of the repartition, in the spectral domain, of the characteristic frequencies of the transitions induced by the different fluctuations rather than by using different correlation times.

Finally we have considered the quadrupolar relaxation of the double- and triple-quantum spectrum. We show that the double-quantum spectrum is composed of two lines whose temperature behavior is similar to the one of the satellites in the monoquantum spectra, while the

TABLE X. Commutators used in the longitudinal quadrupolar relaxation calculations in Sec. III A 1 a.

$[A_0,[A_0,I_z^{cd}]]=0$

$[A_{\mp 1},[A_{\pm 1},I_z^{14}]]=-3[I_z^{14}-I_z^{23}],[A_{\mp 1},[A_{\pm 1},I_z^{23}]]=3[I_z^{14}-I_z^{23}],$

$[A_{\mp 1},[A_{\pm 1},I_z^{12}-I_z^{34}]]=-6[I_z^{12}-I_z^{34}],$

$[A_{\mp 2},[A_{\pm 2},I_z^{14}]]=3[I_z^{14}+I_z^{23}],[A_{\mp 2},[A_{\pm 2},I_z^{23}]]=3[I_z^{14},I_z^{23}],$

$[A_{\mp 2},[A_{\pm 2},I_z^{12}-I_z^{34}]]=6[I_z^{12}-I_z^{34}]$, the A Components are given in Eq. (24).

triple-quantum spectrum has a temperature behavior similar to the central line of the monoquantum spectra.

In this first paper, we restrict our calculations on the quantum part of the relaxation, by choosing on purpose the same monoexponential correlation function for all the fluctuations. In the following paper, we will apply this treatment to some materials of low symmetry in considering a residual nonaveraged perturbation term and in calculating explicitly the correlation functions.

ACKNOWLEDGMENTS

We thank Drs. B. Sapoval, Th. Gobron (Laboratoire de Physique de la Matière Condensée, Ecole Polytechnique, Palaiseau, France) and M. Goldman (Centre d'Etudes Nucléaires de Saclay, Gif-sur-Yvette, France) for very useful discussions. Laboratoire de Physique de la Matière Condensée is Groupe de Recherche No. 38 du Centre National de la Recherche Scientifique.

APPENDIX A

In this appendix we present the commutators used in the calculations of the longitudinal (Table X) and transverse (Table XI) quadrupolar relaxation.

The commutators used in calculations of longitudinal and transverse dipolar (like or unlike) relaxations are obtained similiarly after tedious but straightforward calculations.

APPENDIX B

In this appendix we give the elements of the relaxation matrices for quadrupolar and dipolar fluctuations in presence of a residual time averaged quadrupolar splitting Ω_Q. The notations for the spin-lattice and spin-spin relaxation rates given in the beginning of Tables XII–XVI are the same as in the text. One should note that the slow oscillating terms present in such tables can disappear by changing the variables in the kinetic equations. Introducing the magnetization $\langle u_r^{cd} \rangle$ defined by

TABLE XI. Commutators used in the transverse quadrupolar relaxation calculations in Sec. III A b.

$[A_0,[A_0,I_x^{12}]]=6I_x^{12}$, $[A_0,[A_0,I_x^{23}]]=0$, $[A_0,[A_0,I_x^{34}]]=6I_x^{34}$,

$[A_{\mp 1},[A_{\pm 1},I_x^{12}]]=-3I_{\mp}^{12}$, $[A_{\mp 1},[A_{\pm 1},I_x^{23}]]=-3I_{\pm 1}^{23}$, $[A_{\mp 1},[A_{\pm 1},I_x^{34}]]=-3I_{\mp}^{34}$,

$[A_{\mp 2},[A_{\pm 2},I_x^{12}]]=3[I_x^{12}-I_x^{34}]$, $[A_{\mp 2},[A_{\pm 2},I_x^{23}]]=3I_{\mp}^{23}$,

$[A_{\mp 2},[A_{\pm 2},I_x^{34}]]=3[I_x^{34}-I_x^{12}]$,

$[A_0,[A_0,I_y^{12}]]=6I_y^{12}$, $[A_0,[A_0,I_y^{23}]]=0$, $[A_0,[A_0,I_y^{34}]]=6I_y^{34}$,

$[A_{\mp 1},[A_{\pm 1},I_y^{12}]]=\mp 3iI_{\mp}^{12}$, $[A_{\mp 1},[A_{\pm 1},I_y^{23}]]=\pm 3iI_{\pm}^{23}$,

$[A_{\mp 1},[A_{\pm 1},I_y^{34}]]=-3iI_{\mp}^{34}$

$[A_{\mp 2},[A_{\pm 2},I_y^{12}]]=3[I_y^{12}-I_y^{34}]$, $[A_{\mp 2},[A_{\pm 2},I_y^{23}]]=\pm 3iI_{\mp}^{23}$

$[A_{\mp 2},[A_{\pm 2},I_y^{34}]]=3[I_y^{34}-I_y^{12}]$, the A Components are given in Eq. (24).

TABLE XII. As in Table IV, but modified by the presence of a residual time-averaged quadrupolar splitting Ω_Q.

$$\frac{1}{T_{1Q}^{cd,ef}} = \tfrac{3}{2}C_Q^2[aJ_1(\omega_I-\Omega_Q)+bJ_1(\omega_I+\Omega_Q)+cJ_2(2\omega_I-\Omega_Q)+dJ_2(2\omega_I+\Omega_Q)]$$

cd,ef	a	b	c	d
14,14	1	1	1	1
14,23	−1	−1	1	1
14,12-34	−1	1	−1	1
23,14 = 14,23				
23,23 = 14,14				
23,12-34	1	−1	−1	1
12-34,14	−2	2	−2	2
12-34,23	2	−2	−2	2
12-34,12-34	2	2	2	2

TABLE XIII. As in Table VI, but modified by the presence of a residual time-averaged quadrupolar splitting Ω_Q.

$$\frac{1}{T_{1D_{II}}^{cd,ef}} = \tfrac{1}{3}I(I+1)C_D^2[aJ_0(\Omega_Q)+bJ_0(2\Omega_Q)+cJ_1(\omega_I-\Omega_Q)+dJ_1(\omega_I)+eJ_1(\omega_I+\Omega_Q)$$
$$+fJ_2(2\omega_I-2\Omega_Q)+gJ_2(2\omega_I-\Omega_Q)+hJ_2(2\omega_I)+kJ_2(2\omega_I+\Omega_Q)+lJ_2(2\omega_I+2\Omega_Q)$$

cd,ef	a	b	c	d	e	f	g	h	k	l
14,14	$\frac{1}{10}$		$\frac{3}{8}$		$\frac{3}{8}$	$\frac{9}{20}$	$\frac{3}{10}$	$\frac{9}{10}$	$\frac{3}{10}$	$\frac{9}{20}$
14,23	$-\frac{3}{10}$		$-\frac{3}{8}$		$-\frac{3}{8}$	$-\frac{9}{20}$	$\frac{3}{10}$	$-\frac{9}{10}$	$\frac{3}{10}$	$-\frac{9}{20}$
14,12-34			$-\frac{3}{8}$		$\frac{3}{8}$	$-\frac{9}{20}$	$-\frac{3}{10}$		$\frac{3}{10}$	$\frac{9}{20}$
23,14	$-\frac{3}{10}$		$-\frac{3}{8}$		$-\frac{3}{8}$	$-\frac{9}{20}$	$\frac{3}{10}$	$-\frac{9}{10}$	$\frac{3}{10}$	$-\frac{9}{20}$
23,23	$\frac{9}{10}$		$\frac{3}{8}$	2	$\frac{3}{8}$	$\frac{9}{20}$	$\frac{3}{10}$	$\frac{41}{10}$	$\frac{3}{10}$	$\frac{9}{20}$
23,12-34			$\frac{9}{8}$		$-\frac{9}{8}$	$\frac{27}{80}$	$\frac{9}{40}$		$\frac{9}{40}$	$-\frac{27}{80}$
12−34,14			$-\frac{3}{4}$		$\frac{3}{4}$	$-\frac{9}{10}$	$-\frac{3}{5}$		$\frac{3}{5}$	$\frac{9}{10}$
12−34,23			$\frac{3}{4}$		$-\frac{3}{4}$	$\frac{9}{10}$	$-\frac{3}{5}$		$\frac{3}{5}$	$-\frac{9}{10}$
12−34,12−34	$\frac{1}{5}$	$\frac{3}{10}$	$\frac{3}{4}$		$\frac{3}{4}$	$\frac{9}{10}$	$\frac{3}{5}$		$\frac{3}{5}$	$\frac{9}{10}$

TABLE XIV. As in Table IX, but modified by the presence of a residual time-averaged quadrupole splitting Ω_Q.

$$\frac{1}{T_{1XY}^{cd,ef}} = \sum_{s=+,0,-} a_{XY}^s \frac{1}{T_{1XY,\{+,0,-\}}} \text{ with } X,Y = II \text{ or } IS \text{ and } \{+,0,-\} \Longrightarrow \Omega = \begin{Bmatrix} +\Omega_Q \\ 0 \\ -\Omega_Q \end{Bmatrix}$$

Spin I

$$\frac{1}{T_{1XY,\{+,0,-\}}} = \frac{Z(Z+1)}{3}C_{DIS}^2[a_IJ_0(\omega_I-\omega_S+\Omega)+b_IJ_1(\omega_I+\Omega)+c_IJ_2(\omega_I+\omega_S+\Omega)]$$

$XY\{+,0,-\}$	Z	a_I	b_I	c_I
$II\{+,0,-\}$	S	$\frac{1}{6}$	$\frac{1}{2}$	1
$IS\{+,0,-\}$	I	$-\frac{1}{6}$	0	1

TABLE XIV. (*Continued*).

$\frac{1}{T_{1XY}^{cd,ef}}$	a_{II}^{+}	a_{II}^{0}	a_{II}^{-}	a_{IS}^{+}	a_{IS}^{0}	a_{IS}^{-}
14,14	$\frac{3}{4}$		$\frac{3}{4}$			
14,23	$-\frac{3}{4}$		$-\frac{3}{4}$			
14,12-34	$\frac{3}{4}$		$-\frac{3}{4}$			
14,S_Z				$\frac{3}{20}$		$\frac{3}{20}$
23,14	$-\frac{3}{4}$		$-\frac{3}{4}$			
23,23	$\frac{3}{4}$	4	$\frac{3}{4}$			
23,12-34	$-\frac{3}{4}$		$\frac{3}{4}$			
23,S_z				$-\frac{3}{20}$	$\frac{4}{10}$	$-\frac{3}{20}$
12-34,14	$\frac{3}{2}$		$-\frac{3}{2}$			
12-34,23	$-\frac{3}{2}$		$\frac{3}{2}$			
12-34,12-34	$\frac{3}{2}$		$\frac{3}{2}$			
12-34,S_Z				$\frac{3}{10}$		$-\frac{3}{10}$

Spin S

$$\frac{1}{T_{1XY,\{+,0,-\}}}=\frac{Z(Z+1)}{3}C_{DIS}^{2}[a_S J_0(\omega_S-\omega_I+\Omega)+b_S J_1(\omega_S)+c_S J_2(\omega_I+\omega_S+\Omega)]$$

$XY\{+,0,-\}$	Z	a_S	b_S	c_S
$SI\{+,0,-\}$	S	$-\frac{1}{6}$	0	1
$SS\{+,0,-\}$	I	$\frac{1}{6}$	$\frac{1}{2}$	1

$\frac{1}{T_{1XY}^{cd,ef}}$	a_{SS}^{+}	a_{SS}^{0}	a_{SS}^{-}	a_{SI}^{+}	a_{SI}^{0}	a_{SI}^{-}
S_Z,14	$\frac{3}{2}$					
S_Z,23	$-\frac{3}{2}$	4				
S_Z,12−34	$\frac{3}{2}$		$-\frac{3}{2}$			
S_Z,S_Z				$\frac{3}{10}$	$\frac{2}{5}$	$\frac{3}{10}$

TABLE XV. As in Table V, but modified by the presence of a residual time-averaged quadrupolar splitting Ω_Q. We used below the variables $q^{+}=\exp[2i(\Omega_Q t)_{\text{restr}}]$, $q^{-}=\exp[-2i(\Omega_Q t)_{\text{restr}}]$ where the notation $(\Omega_Q t)_{\text{restr}}$ has been defined in Eqs. (17a), (17b), and (18).

$$\frac{1}{T_{2Q}^{cd,ef}}=C_Q^2[aJ_0(0)+bJ_1(\omega_I-\Omega_Q)+cJ_1(\omega_I+\Omega_Q)+dJ_2(2\omega_I-\Omega_Q)+eJ_2(2\omega_I+\Omega_Q)]$$

cd,ef	a	b	c	d	e
			Single-quantum coherences		
12,12	3	0	3	$\frac{3}{2}$	$\frac{3}{2}$
12,34	0	0	0	$-\frac{3}{2}q^{-}$	$-\frac{3}{2}q^{-}$
23,23	0	$\frac{3}{2}$	$\frac{3}{2}$	$\frac{3}{2}$	$\frac{3}{2}$
34,12	0	0	0	$-\frac{3}{2}q^{+}$	$-\frac{3}{2}q^{+}$
34,34	3	3	0	$\frac{3}{2}$	$\frac{3}{2}$
			Double-quantum coherences		
13,13	3	$\frac{3}{2}$	$\frac{3}{2}$	0	3
13,24	0	$\frac{3}{2}q^{-}$	$\frac{3}{2}q^{-}$	0	0
24,13	0	$\frac{3}{2}q^{+}$	$\frac{3}{2}q^{+}$	0	0
24,24	3	$\frac{3}{2}$	$\frac{3}{2}$	3	0
			Triple-quantum coherence		
14,14	0	$\frac{3}{2}$	$\frac{3}{2}$	$\frac{3}{2}$	$\frac{3}{2}$

TABLE XVI. Dynamical shifts with Ω_Q modification.

	$\omega_Q^{cd,ef}=C_Q^2[bk_1(\omega_I-\Omega_Q)+ck_1(\omega_I+\Omega_Q)+dk_2(2\omega_I-\Omega_Q)+ek_2(2\omega_I+\Omega_Q)]$			
cd,ef	b	c	d	e
		Monoquantum coherences		
12,12	0	6	-3	3
12,34	0	0	$-3q^-$	$3q^-$
23,23	3	3	3	3
34,12	0	0	$3q^+$	$-3q^+$
34,34	6	0	3	-3
		Double-quantum coherences		
13,13	-3	3	0	6
13,24	$3q^-$	$-3q^-$	0	0
24,13	$-3q^+$	$3q^+$	0	0
24,24	3	-3	6	0
		Triple-quantum coherence		
14,14	3	3	3	3

$$\langle u_r^{12}\rangle=\langle I_r^{12}\rangle \exp[i(\Omega_Q t)_{\text{restr}}] , \quad \text{(B1)}$$

$$\langle u_r^{34}\rangle=\langle I_r^{34}\rangle \exp[-i(\Omega_Q t)_{\text{restr}}] . \quad \text{(B2)}$$

one obtains kinetic equations where all the coefficients are constant. According to Eqs. (B1) and (B2) the oscillating terms induce only a splitting of the resonance frequencies.

[1]M. Mehring, *High Resolution NMR in Solids* (Springer Verlag, Berlin 1983); U. Haberlen, *High Resolution in Solids, Selective Averaging* (Academic, New York, 1976); D. Wolf, *Spin Temperature and Nuclear Spin Relaxation in Matter,* (Clarendon, Oxford, 1979), Chap. 12; R. R. Ernst, G. Bodenhausen, and A. Wokaun, *Principles of Nuclear Magnetic Resonance in One and Two Dimensions* (Clarendon, Oxford, 1987).

[2]P. M. Richards, *Physics of Superionic Conductors,* Vol. 15 of *Topics in Current Physics,* edited by M. B. Salamon, (Springer, Berlin, 1979), p. 141; J. L. Bjorkstam and M. Villa, Magn. Res. Rev. **6**, 1 (1980); H. Theveneau, *Structure and Dynamics of Molecular Systems,* edited by R. Daudel, J.-P. Korb, J.-P. Lemaistre, and J. Maruani (Reidel, Dordrecht, 1986), Vol. II, p. 231.

[3]A. Pines, S. Vega, D. J. Ruben, T. W. Shattuck, and D. E. Wemmer, *Magnetic Resonance in Condensed Matter—Recent Developments, Proceedings of the IVth Ampere Summer School, Pula, Yugoslavia,* edited by R. Blinc and G. Lahajnar (J. Stephan Institute, Ljubjana, 1977).

[4]J. Baum, K. K. Gleason, A. Pines, A. N. Garroway, and J. A. Reimer, Phys. Rev. Lett. **56**, 1377 (1986).

[5]R. Kubo and K. Tomita, J. Phys. Soc. Jpn. **9**, 888 (1954).

[6](a) A. Abragam, *The Principles of Nuclear Magnetic Resonance* (Oxford University, London, 1961), Chap. VIII; (b) Chap. VIII, Sec. II F c.

[7]A. G. Redfield, IBM J. **1**, 19 (1957).

[8]E. R. Andrew and D. P. Tunstall, Proc. Phys. Soc. **78**, 1 (1961).

[9]P. S. Hubbard, J. Chem. Phys. **53**, 985 (1970).

[10]M. I. Gordon and M. J. R. Hoch, J. Phys. C **11**, 783 (1978).

[11]B. Halle and H. Wennerström, J. Magn. Reson. **44**, 89 (1981).

[12]A. G. Marshall, J. Chem. Phys. 52, 2527 (1970); T. E. Bull, J. Magn. Reson. **8**, 344 (1972).

[13]C. P. Slichter, *Principles of Magnetic Resonance* (Harper and Row, New York, 1965).

[14]A. Wokaun and R. R. Ernst, Mol. Phys. **36**, 317 (1978).

[15]S. Vega, J. Chem. Phys. **68**, 5518 (1978).

[16]S. Vega and Y. Naor, J. Chem. Phys. **75**, 75 (1981).

[17]D. Petit and B. Sapoval, Solid State Ionics **21**, 293 (1986).

[18]D. Petit, Ph. Colomban, G. Collin, and J.-P. Boilot, Mat. Res. Bull. **21**, 365 (1986).

[19]J.-P. Cohen Addad, J. Chem. Phys. **60**, 2441 (1974).

[20]C. Fouques and L. G. Werbelow, Can. J. Chem. **57**, 2339 (1979); L. G. Werbelow and A. G. Marshall, J. Magn. Reson., 443 (1981).

[21]D. Brinkmann, M. Mali, J. Roos, R. Messer, and H. Birli, Phys. Rev. B **26**, 4810 (1982).

[22]M. H. Cohen and F. Reif, Solid State Phys. **5**, 321 (1957).

[23]J.-P. Korb, M. Winterhalter, and H. M. McConnell, J. Chem. Phys. **80**, 1059 (1984).

[24]L. P. Hwang and J. H. Freed, J. Chem. Phys. **63**, 4017 (1975).

[25]J.-P. Korb, M. Ahadi, G. P. Zientara, and J. H. Freed, J. Chem. Phys. **86**, 1125 (1987); J.-P. Korb, M. Ahadi, and H. M. McConnell, J. Phys. Chem. **91**, 1255 (1987).

[26]D. M. Brink and G. R. Satchler, *Angular Momentum,* (Oxford University Press, London, 1968).

[27]H. Birli, L. Schimmele, and R. Messer, *Proceedings of the XXIInd Ampere Congress, Zurich, 1984,* edited by K. A. Müller, R. Kind, and J. Roos (Schippert & Co., Buchdruck und Offerdruck, Zurich, 1984), p. 171.

[28]D. Petit, Thèse d'Etat, Orsay, 1987.

[29]A. Samoson and E. Lippmaa, Phys. Rev. B **28**, 6567 (1983).

[30]P. P. Man, J. Magn. Reson. **67**, 78 (1986).

[31]S. Vega and A. Pines, J. Chem. Phys. **66**, 5624 (1977).